Report LR-615

Synthesis and Validation of Feedback Guidance Laws for Air-to-Air Interceptions

January 1990

Josef Shinar / Hendrikus G. Visser

TU Delft
Delft University of Technology

Faculty of Aerospace Engineering
Technion-Israel Institute of Technology
Haifa, Israel
Faculty of Aerospace Engineering
Delft, The Netherlands

Synthesis and Validation of Feedback Guidance Laws for Air-to-Air Interceptions

Josef Shinar / Hendrikus G. Visser

ABSTRACT

This report summarizes a multi-year research effort to develop and validate a feedback algorithm for medium-range air-to-air interceptions with realistic capture conditions, compatible with the deployment of advanced guided weapons in a future air combat scenario. In this report a review of previous works as well as some new results are presented.

The proposed guidance algorithm is based on the application of singular perturbation techniques. The algorithm consists of two major elements. A fast converging iterative algorithm provides a three-dimensional "reference flight trajectory" (RFT). It is the solution of a "reduced-order" problem, in which the interceptor velocity vector can be instantaneously oriented towards the optimal direction. The RFT is tracked by using two feedback control laws for steering the velocity vector in horizontal and vertical planes.

The feedback approximation presented herein differs from similar works reported in the open literature by covering all phases of an air-to-air interception, including the terminal "zoom" maneuver. Moreover, at each milestone of the reported multi-year investigation the results obtained by simulating the feedback control laws were compared with "exact" (open-loop) optimal solutions. This process allowed to introduce modifications in the suboptimal control solution leading to a very satisfactory (better than 0.5%) pay-off accuracy.

The examples included in this report, featuring both previous generation (F-4) as well as state-of-the-art (F-15) fighter aircraft models, clearly demonstrate the structural robustness of the feedback guidance laws.

The hierarchical structure of the algorithm, the explicit feedback form of the control laws and the validated high accuracy, make the algorithm a very attractive candidate for a real-time implementation on board of a future interceptor aircraft.

TABLE OF CONTENTS

NOMENCLATURE

C_D	Drag Coefficient
C_{D_0}	Zero-Lift Drag Coefficient
C_L	Lift Coefficient
$C_{L_{max}}$	Maximum Lift Coefficient
d	Effective Firing Range, m
D	Aerodynamic Drag, N
D_i	Induced Drag in Level Flight, N
D_0	Zero-Lift Drag, N
E	Specific Energy, m
$f_{(\bullet)}$, $F_{(\bullet)}$	Function
g	Acceleration due to Gravity, m/s^2
h	Altitude, m
H	Variational Hamiltonian
$I_{(\bullet)}$	Integral
J	Performance Index
L	Aerodynamic Lift, N
M	Mach Number
n	Normal Load Factor
n_h	n sinμ
n_L	Aerodynamic Load Limit
n_{max}	Structural Load Limit
n_v	n cosμ
q	Dynamic Pressure, N/m^2
R	Range, m
S	Wing Surface Area, m^2
t	Time, s
T	Thrust, N
V	Airspeed, m/s
W	Aircraft Weight, N
x	Down-Range, m
y	Cross-Range, m

γ ..... Flight-Path Angle, rad

Δh ..... $h - h_T$, m

ε ..... Singular Perturbation Parameter

η ..... Throttle Setting

θ ..... Line-of-Sight Angle in the Vertical Plane, rad

$\lambda_{(\bullet)}$ ..... Adjoint Variable

μ ..... Bank Angle, rad

ν ..... Multiplier

ρ ..... Air Density (kg/m^3)

τ ..... Stretched Time

χ ..... Heading Angle, rad

ψ ..... Line-of-Sight Angle in the Horizontal Plane, rad

Subscripts:

$(\bullet)_0$ ..... Initial Value

$(\bullet)_1$ ..... First Boundary Layer

$(\bullet)_2$ ..... Second Boundary Layer

$(\bullet)_f$ ..... Final Value

$(\bullet)_{max}$ ..... Maximum Value

$(\bullet)_{min}$ ..... Minimum Value

$(\bullet)_T$ ..... Target

$(\bullet)_u$ ..... Unconstrained Optimal Value

Superscripts:

$(\bullet)^1$ ..... First Boundary Layer

$(\bullet)^2$ ..... Second Boundary Layer

$(\bullet)^b$ ..... Boundary Layer

$(\bullet)^r$ ..... Reduced-Order

$(\bullet)^z$ ..... Zoom

This report was prepared during the Sabbatical leave of Prof. Josef Shinar, from the Faculty of Aerospace Engineering, Technion - Israel Institute of Technology, Haifa, Israel, being invited as a Visiting Professor at the Faculty of Aerospace Engineering, Delft University of Technology, Delft, The Netherlands.

This report is dedicated to the memory of Prof. H.J. Kelley, whose ideas have inspired both authors.

I. INTRODUCTION

Interception of adversary aircraft with the objective to disrupt a hostile mission has been a basic air-to-air task since the very first years of air warfare. Not surprisingly, this task has spurred a continuous research effort as a part of evaluating air-to-air combat performance of fighter aircraft. The assumption of a known adversary trajectory allows to formulate the interception as a minimum-time optimal control problem. Simplified analysis [1, 2] indicates that the optimal trajectory of the interceptor has three distinct phases:

(i) an initial turn-climb-acceleration phase,

(ii) a steady-state cruise at maximum speed,

(iii) an end-game terminating with capture as determined by the weapon of the interceptor.

Such a decomposition is valid only if the initial conditions of the encounter allow the interceptor to reach its maximum speed before the end-game is initiated, a condition generally satisfied in long-range interceptions. For shorter ranges, phase (ii) disappears and the initial and terminal parts of the trajectory are merged together. The optimal control solution associated with such a trajectory is generally obtained in an open-loop form by solving a high dimensional nonlinear two-point-boundary-value problem using some iterative algorithm.

For a real-time airborne application, as well as for a systematic performance assessment, a reasonably accurate feedback approximation of the optimal control solution is more useful. This challenge drew a considerable interest for investigations in the last decade. The first works [3, 4] were oriented towards long-range interceptions of low flying targets with the requirement of point capture. Later extensions included medium-range scenarios, characterized by the absence of the dash segment [5], validation by ground based pilot-in-the-loop simulations [6] and some flight testing [7]. These last activities [6,7] provided an encouraging proof of feasibility for such algorithms. Unfortunately, however, the accuracy of the guidance algorithm derived in [5] by applying singular perturbation methods, has never been tested.

The objective of this Chapter is to summarize a multi-year joint effort of the authors to develop and validate a feedback algorithm for medium-range air-to-air interceptions with realistic capture conditions compatible with the deployment of advanced guided weapons in a future air combat. This effort was based, similarly to [3-7], on a singular perturbation approach, but used a different multiple time-scale model. Moreover, at each milestone during the development of the algorithm, a special effort

was undertaken to compare the outcome of the feedback approximations to the optimal control solution. In the open literature only a single similar study of limited scope [8] is known. In the first phase, horizontal [9,10] and vertical [11,12] interceptions were analyzed separately, leading to an enhanced insight into the problems associated with each planar maneuver. The feedback guidance law for a three-dimensional interception was then synthesized based on a vectorial combination of the two-dimensional controls and compared to the results of open-loop optimal control solutions [13,14].

This Chapter includes a review of previous works [9-14], as well as some new results and is organized as follows. In Section II the detailed mathematical formulation of the problem is presented and the formal optimal control solution is derived. In Section III modeling considerations and the application of singular perturbation theory for approximating the optimal control in feedback form are outlined. In Section IV the interception in the horizontal plane is analyzed and a uniformly valid feedback guidance law is derived. In section V the problems of the interception in a vertical plane are discussed and the synthesis of the resulting feedback guidance law is presented. It is followed in Section VI by the description of the problems involved in the synthesis of a three-dimensional feedback control strategy and a new numerical example, in which the simulated feedback approximation is compared with the open-loop optimal solution, using an aircraft model representative of a state-of-the-art high-performance fighter interceptor.

II. PROBLEM FORMULATION

A. MATHEMATICAL MODEL

The air-to-air interceptions analyzed in this chapter are characterized by the following features:

(i) The adversary aircraft (target) is assumed to fly at a fixed altitude and direction with constant speed.

(ii) The initial distance of separation is large compared with the turning radius of the interceptor, but not large enough to allow the interceptor to reach its maximum speed. This last statement defines the domain of "medium-range" interceptions.

(iii) The interception terminates when the distance of separation becomes equal to the effective firing range of the interceptor weapon (assumed to be an air-to-air missile).

In a Cartesian coordinate system, centered at the target (T) and with the x-axis is aligned with its velocity vector, the equations of relative motion (see Fig.1 for the definition of the variables) are given by:

$$\dot{x} = V\cos\gamma\cos\chi - V_T \triangleq F_x \quad , \quad x(t_0) = x_0 \tag{1}$$

$$\dot{y} = V\cos\gamma\sin\chi \triangleq F_y \quad , \quad y(t_0) = y_0 \tag{2}$$

$$\dot{\Delta h} = \dot{h} = V\sin\gamma \triangleq F_h \quad , \quad \Delta h(t_0) = h(t_0) - h_T = \Delta h_0 \tag{3}$$

The dynamic model of the interceptor assumes a flat non-rotating earth, point-mass approximation and thrust aligned with the velocity vector. The corresponding equations of motion are:

$$\dot{V} = g[(T-D)/W - \sin\gamma] \triangleq F_V \quad , \quad V(t_0) = V_0 \tag{4}$$

$$\dot{\gamma} = (g/V)[(L/W)\cos\mu - \cos\gamma] \triangleq F_\gamma \quad , \quad \gamma(t_0) = \gamma_0 \tag{5}$$

$$\dot{\chi} = (g/V\cos\gamma)[(L/W)\sin\mu] \triangleq F_\chi \quad , \quad \chi(t_0) = \chi_0 \tag{6}$$

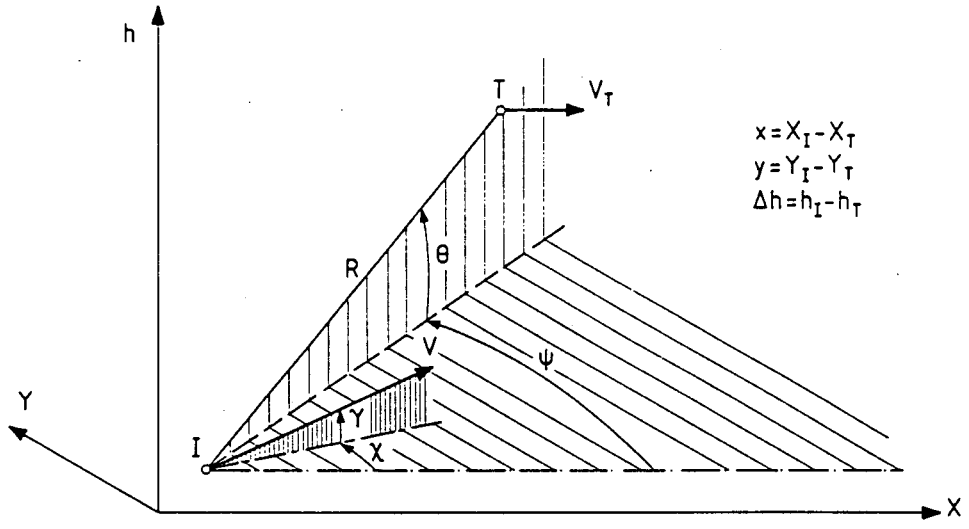

Fig. 1 Three-dimensional Interception Geometry.

The aerodynamic forces (lift and drag) and the maximum available thrust are functions of speed and altitude:

$$L = 0.5\rho(h)V^2SC_L \tag{7}$$

$$D = 0.5\rho(h)V^2SC_D \tag{8}$$

$$T = \eta T_{max}(h,V) \tag{9}$$

Based on the definition of the aerodynamic load factor:

$$n \triangleq (L/W) \tag{10}$$

and assuming a parabolic drag polar, the total drag force can be expressed as:

$$D = D_0 + n^2 D_i = D(h,V,n) \quad , \tag{11}$$

where the zero-lift drag and the induced drag in level flight (n=1) are defined respectively by:

$$D_0 = 0.5\rho V^2 S C_{D_0} \tag{12}$$

$$D_i = 2KW^2/(\rho V^2 S) \quad , \tag{13}$$

The non-dimensional coefficients C_{D_0} and K are functions of Mach number. In this mathematical model the controls are:

(i) The throttle parameter η constrained by:

$$0 \leq \eta \leq 1 \tag{14}$$

(ii) The bank angle μ which determines the direction of the lift force.

(iii) The aerodynamic load factor n defined by Eq.(10). It is subject to two different constraints: a structural limit which is effective at high speeds:

$$|n| \leq n_{max} \tag{15}$$

and a limit imposed by the maximum lift coefficient:

$$|n| \leq n_L(h,V) \triangleq \frac{0.5\rho V^2 S}{W} C_{L_{max}}(M) \tag{16}$$

Quite often it is convenient to use as controls the horizontal and vertical components of the load factor, defined by:

$$n_h \triangleq n \sin\mu \tag{17}$$

$$n_v \triangleq n \cos\mu \tag{18}$$

The interceptor's trajectory has to be confined, as any other maneuver, to the flight envelope of the aircraft, determined by the following state constraints:

$$0 < h_{min} \leq h \leq h_{max} \tag{19}$$

$$V_{min}(h) \leq V \leq V_{max}(h) \tag{20}$$

B. OPTIMAL CONTROL FORMULATION

For the sake of a concise formulation let us define the state vector of the three-dimensional interception problem as:

$$\underline{X}^T \triangleq (x,\ y,\ \Delta h,\ V,\ \gamma,\ \chi) \tag{21}$$

The optimal control problem to be solved is to determine the control vector $\underline{U}^{*T} \triangleq (n^*,\ \mu^*,\ n^*)$ that brings the interceptor from a given set of initial conditions $\underline{X}(t_0)$ to a terminal manifold, - which depends on the effective weapon firing envelope, - in the shortest possible time, subject to the state and control constraints. The performance index is therefore the final time:

$$J = \int_{t_0}^{t_f} dt = t_f \quad , \tag{22}$$

defined by the terminal manifold:

$$t_f = \arg \{ \Phi[t_f, \underline{X}(t=t_f)] = 0 \} \tag{23}$$

The variational Hamiltonian of this problem is:

$$H = -1 + \underline{\lambda} \cdot \dot{\underline{X}} + \text{constraints} = H(\underline{X}, \underline{\lambda}, \underline{U}) \quad , \tag{24}$$

where the costate vector $\underline{\lambda}$ has to satisfy the adjoint equations:

$$\dot{\underline{\lambda}} = - \frac{\partial H}{\partial \underline{X}} \tag{25}$$

and the corresponding transversality conditions:

$$\underline{\lambda}(t_f) = \nu \left. \frac{\partial \Phi}{\partial \underline{X}} \right|_{t=t_f} \quad , \tag{26}$$

where ν is a Lagrange multiplier.

According to the Maximum Principle the optimal controls have to maximize the Hamiltonian:

$$\underline{U}^* = \arg \max_{\underline{U}} H(\underline{X}, \underline{\lambda}, \underline{U}) \tag{27}$$

Moreover, since time does not appear explicitly in the equations and the final time is not specified:

$$H^* \triangleq H(\underline{X}, \underline{\lambda}, \underline{U}^*) = H\Big|_{t_f} = 0 \tag{28}$$

This formulation requires to solve a nonlinear two-point-boundary-value problem of 12 dimensions, resulting in $\underline{X}^*(t)$, $\underline{\lambda}^*(t)$ and consequently $\underline{U}^*(t)$. A feedback approximation of the optimal control can be obtained if one can approximate the adjoint variables by explicit functions of the state variables. One approach to carry out such an operation is the application of singular perturbation theory, as outlined in the next section.

III. APPLICATION OF SINGULAR PERTURBATION THEORY

A singular perturbed dynamic system is characterized by a small parameter ε, multiplying the time derivatives of some components of the state vector. These components behave as "fast" variables compared to the other part of the state vector. This indicates that the mathematical structure of singularly perturbed systems is always associated with the physical phenomenon of time-scale separation. Singularly perturbed mathematical models are frequently encountered in celestial mechanics, fluid dynamics, physical chemistry etc. and have been subjects of thorough investigations [15-19]. The basic approach to solve singular perturbation problems, formulated as initial value problems, has been the method of Matched Asymptotic Expansions [20, 21]. This method was also extended to deal with two-point boundary-value problems and adapted to solve optimal control problems as well [22-26].

If one sets in a singular perturbation problem $\varepsilon = 0$, the "fast" dynamics are neglected and the order of the dynamic system is reduced. The solution of the "reduced-order" system may serve as an approximation, though it cannot satisfy the initial and terminal conditions imposed on the "fast" variables. This deficiency is corrected by initial and terminal "boundary-layer" solutions computed on a stretched time-scale. Expanding all variables in both the original and the boundary-layer problems in asymptotic power series of ε and matching the corresponding terms lead to a uniformly valid "composite solution" of the problem. Using only a finite number of terms of the expansions yields an approximation. The optimal control solution approximated by this method is obtained in an open-loop form. It was, however, found [23, 27-28] that if the terminal constraints do not involve the "fast" variables, the terminal "boundary-layer" may disappear and in this case the optimal control approximation can be expressed

in a feedback form. This result, which is very attractive for real-time on-line applications, was recently confirmed [29] by demonstrating that under certain conditions, the optimal feedback control solution of a singularly perturbed system can be constructed, - by a recursive solution of the Hamilton-Jacobi-Bellman equation, - as a single and uniformly valid expansion of the parameter ε.

The application of singular perturbation theory to optimize aircraft trajectories is based on identifying the actual time-scale separations between the state variables. In a linear time-invariant system such time-scale separation can be expressed by the ratio of the respective eigenvalues, which in some case is a small parameter. An appropriate scaling transformation results in multiplying the derivative of the "fast" variable by this small parameter. In the strongly nonlinear problems encountered in flight mechanics the identification of a small parameter associated with the observed time-scale separation is, unfortunately, rather difficult. For this reason it was proposed [30] to insert the singular perturbation parameter ε artificially by multiplying the observed "fast" time derivatives. This approach, called in some papers [9-14] a "forced singular perturbation" technique (FSP), has been used in most aircraft performance optimization studies [3-14, 27]. In [28] it was formally demonstrated that the zeroth-order feedback control approximation of an FSP problem is identical to the solution of a similar classical SP problem obtained by a scaling transformation. Moreover, this result was later extended to higher order corrections [31,10].

The application of the FSP technique for obtaining a zeroth-order feedback control approximation can be summarized by the following steps:

1. Order the state variables according to their relative rate of change (the faster following the slower). This first

step is of major importance and the key to a satisfactory result.

2. Transform the set of original state equations to a singularly perturbed multiple time-scale dynamic model by multiplying the time derivatives of the "fast" variables of the same time-scale by increasing powers of ϵ. It is preferable to have only a single (active) variable on the same time-scale.
3. Set $\epsilon = 0$ and solve the resulting "reduced-order" optimal control problem. In this "reduced-order" solution the "fast" variables play the role of pseudo-controls, constrained to an "integral manifold". Thus, the controls, as well as the respective costate variables are functions of the "slow" state variables only.
4. Solve the first "boundary layer" problem by a time-scale stretching transformation. In this stretched time-scale the "slow" variables are frozen to their initial values. The major element in the solution is to express the active costate variable as a function of the active state variable and the frozen initial values of the "slow" states.
5. Repeat this step for all "boundary layers". It will finally result in approximating all costate variables by a feedback type expression as functions of the "frozen" initial states and the active state.
6. Find the expression for the control variables in the last (fastest) "boundary layer" at the initial time. This expression will be a function of the initial conditions only.
7. Since any current state can be considered as a new set of initial conditions, a uniformly valid feedback control law can be synthesized by replacing the initial values of the state variables with the current values.

The method for higher order corrections is similar, however the matching process is far more elaborate. For details the reader is referred to [31].

Since the application of the above outlined method to the problem of a three-dimensional air-to-air interception involves very complex modeling considerations, in the next sections the more simple planar geometries are analyzed.

IV. INTERCEPTION IN A HORIZONTAL PLANE

A. FORMULATION OF THE HORIZONTAL INTERCEPTION PROBLEM

1. DYNAMIC EQUATIONS

For the restricted case of flight in a horizontal plane ($F_h = 0 \rightarrow \gamma = 0$), it is sometimes more convenient to describe the relative motion between the two aircraft in polar coordinates, using the distance of separation R and the line-of-sight angle ψ:

$$\dot{R} = V_T\cos\psi - V\cos(\psi - \chi) \triangleq f_R(\psi,V,\chi) \tag{29}$$

$$\dot{\psi} = [- V_T\sin\psi + V\sin(\psi - \chi)]/R \triangleq f_\psi(R,\psi,V,\chi) \tag{30}$$

The condition of vertical force equilibrium, obtained by substituting in Eq.(5) $\gamma = F_\gamma = 0$, relates the bank angle μ to the load factor n by:

$$n = 1/\cos\mu \quad , \tag{31}$$

allowing to eliminate the load factor n from the problem formulation. As a consequence, the equations of motion (4) and (6) reduce to:

$$\dot{V} = (g/W)[\eta T_{max} - D_o - (1 + \tan^2\mu)D_i] \triangleq f_V(\eta,V,\mu) \tag{32}$$

$$\dot{\chi} = (g/V)\tan\mu \triangleq f_\chi(V,\mu) \tag{33}$$

In this formulation the interceptor's motion is governed by two independent control variables, the throttle parameter η and the bank angle μ. The maximum admissible value of the bank angle is determined by the load factor constraints given by Eqs.(15)-(16), i.e.:

$$|\mu| \leq \mu_{max} , \tag{34}$$

where:

$$\mu_{max} = \sec^{-1}\{ \min [n_L, n_{max}] \} \tag{35}$$

2. OPTIMAL CONTROL FORMULATION

The variational Hamiltonian for the horizontal problem is:

$$H = -1 + \lambda_R f_R + \lambda_\psi f_\psi + \lambda_V f_V + \lambda_\chi f_\chi + \text{constraints} \tag{36}$$

The adjoint differential equations and the corresponding transversality conditions are:

$$\dot{\lambda}_R = -\frac{\partial H}{\partial R} \tag{37}$$

$$\dot{\lambda}_\psi = -\frac{\partial H}{\partial \psi} , \qquad \lambda_\psi(t_f) = 0 \tag{38}$$

$$\dot{\lambda}_V = -\frac{\partial H}{\partial V} , \qquad \lambda_V(t_f) = 0 \tag{39}$$

$$\dot{\lambda}_\chi = -\frac{\partial H}{\partial \chi} , \qquad \lambda_\chi(t_f) = 0 \tag{40}$$

Assuming that an optimal control solution exists, the Maximum Principle can be used to express the optimal controls in terms of the state and adjoint variables:

$$\lambda_V > 0 : \quad \eta^* = 1 \quad , \quad \mu^* = \min [\ |\mu_u|, \mu_{max}]\ \text{sign}(\lambda_\chi) \tag{41}$$

$$\lambda_V < 0 : \quad \eta^* = 0 \quad , \quad \mu^* = \mu_{max}\ \text{sign}(\lambda_\chi) \ , \tag{42}$$

where μ_u is the unconstrained optimal bank angle, given by:

$$\mu_u = \arctan\left(\frac{\lambda_\chi}{\lambda_V} \frac{W}{2VD_i} \right) \tag{43}$$

A singular throttle arc, along which $\lambda_V = 0$ over a non-zero time interval, is likely to occur in isolated situations only [30,32].

Since time does not appear explicitly in the equations and the final time is not specified, one also has:

$$H^* = H\Big|_{t_f} = 0 \tag{44}$$

Substantial simplification of the two-point-boundary-value problem is obtained by closed-form integration of the adjoint equations [32]. It is readily verified that the solutions to Eqs.(37)-(40) are:

$$\lambda_R = \frac{\cos(\psi - \psi_f)}{f_R(\psi_f, V_f, \chi_f)} \tag{45}$$

$$\lambda_\psi = - \frac{R \sin(\psi - \psi_f)}{f_R(\psi_f, V_f, \chi_f)} \tag{46}$$

$$\lambda_V f_V(\eta, V, \mu) = - \left[\lambda_\chi f_\chi(V, \mu) + \frac{V_f \cos(\psi_f - \chi_f) - V \cos(\psi_f - \chi)}{f_R(\psi_f, V_f, \chi_f)} \right] \tag{47}$$

$$\lambda_\chi = \frac{R \sin(\psi - \psi_f) - V_T \sin\psi_f (t_f - t)}{f_R(\psi_f, V_f, \chi_f)} \tag{48}$$

The special case $\dot{\lambda}_\chi = \lambda_\chi = 0$ is of particular interest. Substitution of Eqs.(45)-(46) into Eq.(40) shows that:

$$\dot{\lambda}_\chi = -\frac{\partial H}{\partial \chi} = \frac{V \sin(\psi_f - \chi)}{f_R(\psi_f, V_f, \chi_f)} \tag{49}$$

From Eqs.(49) and (43) it is then clear that in this case the extremal is a straight line given by:

$$\chi = \psi_f = \text{constant} \tag{50}$$

If $\lambda_V > 0$, this straight-line trajectory is flown with full throttle and zero bank angle. However, the possibility of a zero-throttle bank angle chattering arc arises if $\lambda_V < 0$.

The quantities λ_V and λ_χ in Eqs.(41)-(43) vanish at the final time. Thus the control at t_f depends upon the derivatives of these quantities. Taking the limit in Eq.(43) as $t \to t_f$ results in:

$$\lim_{t \to t_f} \mu_u = \arctan\left[\frac{W}{2D_i} \tan(\psi_f - \chi_f)\right] \tag{51}$$

Due to the dependence on the unspecified terminal quantities ψ_f, V_f, χ_f and t_f, the optimal control law can not be implemented in a feedback form. Extremal trajectories can be generated only by backward integration for an assumed termination of the encounter. For a medium-range scenario, such extremals can be characterized as consisting of a turning phase followed by a phase of acceleration. During the initial phase the interceptor executes a hard turn to the direction of the final line-of-sight, possibly decelerating in the process. Then in the second phase the interceptor accelerates to the final velocity, flying a

nearly straight line trajectory at full throttle. It is evident from Eq.(51) that for this type of engagement the final parameters ψ_f and χ_f must be selected such that the absolute value of the difference of the two is very small. Recall from Eq.(50), that if $\psi_f = \chi_f$, a degenerated straight-line extremal is obtained.

In order to obtain an approximation of the optimal control in feedback form for the variable speed horizontal interception problem, the method of forced singular perturbation is applied.

B. SINGULAR PERTURBATION ANALYSIS

1. MODELING CONSIDERATIONS

The success of the singular perturbation approach depends largely on the ability to identify time-scale separations of the state variables. The assessment of the time-scale separations is largely based on an understanding of the system's dynamic behavior, depending on such factors as aerodynamic characteristics, engine performance, vehicle weight, atmospheric conditions, capture conditions and the initial conditions of the encounter. It has to be noted that different assumptions concerning the system's dynamic behavior, may lead to a different ordering of the dynamics. For instance, in [34] velocity is assumed to be the fastest variable of all. This particular ordering implies sufficient control over velocity, i.e. a very high thrust to weight ratio, and is therefore appropriate mostly for rocket propelled vehicles. The time-scale selection employed here is based on the following observations:

- In a medium-range scenario, the initial separation distance is relatively large and therefore the rate of change in the direction of the line-of-sight will be slow compared with the turning rate of the interceptor.
- Longitudinal accelerations of a fighter aircraft are

generally much smaller than the lateral accelerations used for turning.

- The equations describing the relative motion of the two aircraft in polar coordinates are highly coupled and should therefore be analyzed on the same time-scale.

By assuming the velocity dynamics to be faster than the relative position dynamics, a rather simple closed-form feedback solution can be obtained [9]. This formulation requires the initial conditions of the encounter to be such as to allow the interceptor to reach maximum speed. Unfortunately, even for high-performance fighters the assumed time-scale separation can not be warranted for all initial conditions of interest. Hence this formulation does not apply to a medium-range scenario as defined in Section II,A.

Based on the above it seems appropriate that for the variable speed medium-range horizontal interception problem the state variables R, ψ, V are considered on the same "slow" time-scale, while χ is designated the role of "fast" variable.

The dynamic equations and boundary conditions associated with the singularly perturbed dynamic model selected here, are:

$$\dot{R} = f_R(\psi,V,\chi) \quad , \qquad R(t_0) = R_0 \quad , \quad R(t_f) = d \tag{52}$$

$$\dot{\psi} = f_\psi(R,\psi,V,\chi) \quad , \qquad \psi(t_0) = \psi_0 \tag{53}$$

$$\dot{V} = f_V(n,V,\mu) \quad , \qquad V(t_0) = V_0 \tag{54}$$

$$\varepsilon\dot{\chi} = f_\chi(V,\mu) \quad , \qquad \chi(t_0) = \chi_0 \tag{55}$$

The system of adjoint equations and corresponding transversality conditions may be written as:

$$\dot{\lambda}_R = -\frac{\partial H}{\partial R} \tag{56}$$

$$\dot{\lambda}_{\psi} = -\frac{\partial H}{\partial \psi} \quad , \qquad \lambda_{\psi}(t_f) = 0 \tag{57}$$

$$\dot{\lambda}_{V} = -\frac{\partial H}{\partial V} \quad , \qquad \lambda_{V}(t_f) = 0 \tag{58}$$

$$\varepsilon\dot{\lambda}_{\chi} = -\frac{\partial H}{\partial \chi} \quad , \qquad \lambda_{\chi}(t_f) = 0 \quad , \tag{59}$$

where H remains as defined in Eq.(36). The optimality conditions given by Eqs.(41)-(44) also remain unchanged in the singular perturbation formulation.

A detailed analysis leading to the derivation of a feedback guidance law based on the above FSP model is presented in [10] and is briefly reviewed in the next subsection.

2. HORIZONTAL GUIDANCE LAW SYNTHESIS

Taking the limit in Eqs.(55) and (59) as $\varepsilon \to 0$, the following necessary conditions for optimality of the "reduced-order" solution are obtained:

$$\mu^r = 0 \quad , \qquad \frac{\partial H^r}{\partial \chi} = -\frac{V^r \sin(\psi_f^r - \chi^r)}{f_R(\psi_f^r, V_f^r, \chi_f^r)} = 0 \quad , \tag{60}$$

where superscript "r" is used to denote the "reduced-order" solution. Note from Eq.(60), that in the "reduced-order" problem χ takes on the role of control variable, whereas the original control μ now becomes a constraint. It is clear, that the optimal trajectory of the interceptor in the "reduced-order" problem is a straight line. The optimal heading χ^r is readily found from Eq.(60):

$$\chi^r = \psi_f^r = \text{constant} \tag{61}$$

Though the "reduced-order" system of state equations is three-dimensional, the optimal direction χ^r of the straight-line trajectory can be solved in terms of the initial state with a minimal computational effort, compatible with real-time requirements. To support the development of a geometrical solution for the reduced-order problem (see Fig.2), the following integrals are introduced:

$$I_t(V_0, V_f) \triangleq \int dt = \int_{V_0}^{V_f} \frac{dt}{dV}\, dV = \int_{V_0}^{V_f} \frac{(W/g)}{(T_{max} - D_0 - D_i)}\, dV \qquad (62)$$

$$I_s(V_0, V_f) \triangleq \int V dt = \int_{V_0}^{V_f} V \frac{dt}{dV}\, dV = \int_{V_0}^{V_f} \frac{V(W/g)}{(T_{max} - D_0 - D_i)}\, dV \qquad (63)$$

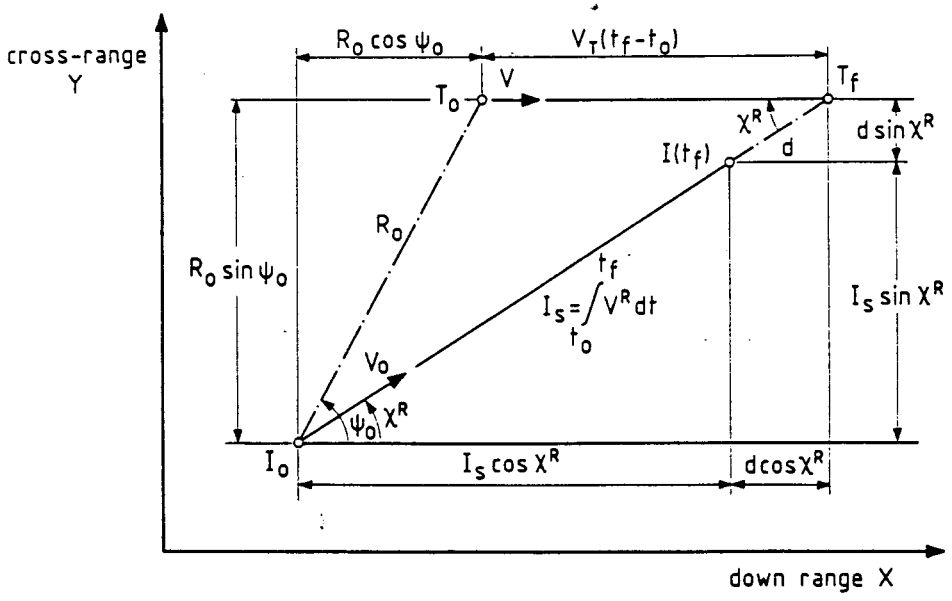

Fig. 2. "Reduced-order" Solution in the Horizontal Plane.

Equations (62)-(63) give the time and distance needed by the interceptor to reach the velocity V_f starting at V_0, while flying a straight line trajectory. Based on these expressions, the interception geometry can be solved in Cartesian coordinates:

$$x(t_f) = d\cos\chi^r = R_0\cos\psi_0 + I_t(V_0, V_f^r)V_T - I_s(V_0, V_f^r)\cos\chi^r \tag{64}$$

$$y(t_f) = d\sin\chi^r = R_0\sin\psi_0 - I_s(V_0, V_f^r)\sin\chi^r \tag{65}$$

Equations (64)-(65) can be solved by a simple one-dimensional search, yielding both V_f^r and χ^r in terms of the initial conditions (R_0, ψ_0, V_0):

$$V_f^r = \bar{V}_f(R_0, \psi_0, V_0) \ , \qquad \chi^r = \bar{\chi}(R_0, \psi_0, V_0) \tag{66}$$

Based on Eqs.(66) and (61), the "reduced-order" solution can be completed by evaluating the initial values of the "slow" adjoints, using Eqs.(45)-(47):

$$\lambda_R^r(t_0) = \frac{\cos[\psi_0 - \bar{\chi}(R_0, \psi_0, V_0)]}{V_T\cos[\bar{\chi}(R_0, \psi_0, V_0)] - \bar{V}_f(R_0, \psi_0, V_0)} \triangleq \bar{\lambda}_R(R_0, \psi_0, V_0) \tag{67}$$

$$\lambda_\psi^r(t_0) = \frac{-R_0\sin[\psi_0 - \bar{\chi}(R_0, \psi_0, V_0)]}{V_T\cos[\bar{\chi}(R_0, \psi_0, V_0)] - \bar{V}_f(R_0, \psi_0, V_0)} \triangleq \bar{\lambda}_\psi(R_0, \psi_0, V_0) \tag{68}$$

$$\lambda_V^r(t_0) = \frac{V_0 - \bar{V}_f(R_0, \psi_0, V_0)}{V_T\cos[\bar{\chi}(R_0, \psi_0, V_0)] - \bar{V}_f(R_0, \psi_0, V_0)} \frac{W/g}{[T_{max} - D_0 - D_i]_0}$$

$$\triangleq \bar{\lambda}_V(R_0, \psi_0, V_0) \tag{69}$$

The boundary-layer system (denoted by superscript "b") is obtained by introducing the time transformation:

$$\tau = (t - t_0)/\varepsilon \quad , \tag{70}$$

into the original system given by Eqs.(52)-(59), yielding:

$$\frac{dR^b}{d\tau} = \varepsilon f_R(\psi,V,\chi) \tag{71}$$

$$\frac{d\psi^b}{d\tau} = \varepsilon f_\psi(R,\psi,V,\chi) \tag{72}$$

$$\frac{dV^b}{d\tau} = \varepsilon f_V(n,V,\mu) \tag{73}$$

$$\frac{d\chi^b}{d\tau} = f_\chi(V,\mu) \tag{74}$$

$$\frac{d\lambda_R^b}{d\tau} = -\varepsilon\frac{\partial H}{\partial R} \tag{75}$$

$$\frac{d\lambda_\psi^b}{d\tau} = -\varepsilon\frac{\partial H}{\partial \psi} \tag{76}$$

$$\frac{d\lambda_V^b}{d\tau} = -\varepsilon\frac{\partial H}{\partial V} \tag{77}$$

$$\frac{d\lambda_\chi^b}{d\tau} = -\frac{\partial H}{\partial \chi} \tag{78}$$

In the zeroth order boundary-layer approximation, obtained by setting $\varepsilon = 0$ in Eqs.(71)-(78), all "slow" state variables (R^b,ψ^b,V^b) and corresponding adjoints $(\lambda_R^b,\lambda_\psi^b,\lambda_V^b)$ remain frozen at their initial values at $\tau = 0$. Moreover, according to the Matching Principle [25], these values have to be equal to the initial values of the "reduced-order" solution, i.e.:

$$R^b(\tau) = R_0 \quad , \quad \psi^b(\tau) = \psi_0 \quad , \quad V^b(\tau) = V_0 \tag{79}$$

$$\lambda_R^b(\tau) = \lambda_R^r(t_0) \quad , \quad \lambda_\psi^b(\tau) = \lambda_\psi^r(t_0) \quad , \quad \lambda_V^b(\tau) = \lambda_V^r(t_0) \tag{80}$$

Substitution of Eqs.(79), (80) and (67)-(69) into Eq.(44), allows the "fast" heading adjoint in the turning boundary layer $\lambda_\chi^b(\tau)$ to be expressed in terms of the initial "slow" states, the active state $\chi^b(\tau)$ and the control $\mu^b(\tau)$. Assuming unconstrained control for $\tau = 0$, substitution of this result into the optimal control solution given by Eqs.(41)-(43), yields the following expression for the optimal bank angle in the boundary layer:

$$\tan \mu^b(0) = \tan\mu_{ss}(V_0) \times \left[\frac{2V_0}{\bar{V}_f(R_0, \psi_0, V_0) - V_0}\right]^{1/2} \sin\left[\frac{\bar{\chi}(R_0, \psi_0, V_0) - \chi_0}{2}\right]$$

$$= \tan\bar{\mu}(R_0, \psi_0, V_0, \chi_0) \quad , \tag{81}$$

where:

$$\tan\mu_{ss}(V_0) = \left[\frac{T_{max} - D_0}{D_i} - 1\right]^{1/2} \quad , \tag{82}$$

is the bank angle for a steady-state horizontal turn.

A uniformly valid zeroth-order feedback law can be synthesized by merely replacing the initial state by the current state.

3. DISCUSSION

Analysis of singular perturbation approximate solutions reveals a characteristic behavior very similar to that of open-loop extremals for medium-range scenario's. Both the exact and the approximate control strategies are characterized by a

gradually decreasing rate-of-turn as the flight direction asymptotically reaches its reference value. The main difference between the two control strategies is the reference direction. In the singular perturbation solution the final line-of-sight angle, which is the reference direction in the exact solution, is approximated by the instantaneous collision course. The larger the difference between the instantaneous collision course and the final line-of-sight angle, the worse the accuracy of the singular perturbation approximation. Obviously, a large difference is merely a reflection of a lack of "true" time-scale separation.

The guidance law derived in [9] (and also used in [11] and [13]), which is based on treating the velocity dynamics on a separate intermediate time-scale, exhibits great similarity with the guidance law given by Eq.(81). In fact, the guidance laws are the same, except that in [9] the reference velocity $\bar{V}_f(R,\psi,V)$ is replaced by the maximum velocity and the reference direction $\bar{\chi}(R,\psi,V)$ is replaced by the so-called "modified collision course". It is evident that the performance of this guidance law suffers substantially in encounters where the initial separation distance is not sufficiently large to permit the interceptor to attain maximum velocity.

C. NUMERICAL EXAMPLES

In order to evaluate the accuracy of the zeroth-order feedback strategy and the possible need for first-order corrections, two numerical examples are considered. In both examples the approximate feedback solutions are compared with the respective open-loop extremal solutions. The first example is typical of a medium-range scenario. The boundary conditions, the selected parameters and some characteristic results for this example are summarized in Table 1. The geometric perturbation parameter ε_g, borrowed from the constant-speed interception problem [9,28,31],

is introduced in Table 1 to serve as a measure of time-scale separation.

Although for the presented example the accuracy of the guidance law of Eq.(81) is more than adequate, improvements may be called for in case of relatively short-range engagements. Such improvements can be obtained by incorporating first-order correction terms in the singular perturbation control approximation.

The only difference between the exact optimal solution and the zeroth-order singular perturbation approximation is that in the singular perturbation approach the slow adjoints $(\lambda_R, \lambda_\psi, \lambda_V)$ are approximated by the "reduced-order" feedback expressions $(\bar{\lambda}_R, \bar{\lambda}_\psi, \bar{\lambda}_V)$. Thus, improving the approximate feedback control solution implies improving the estimates of the slow adjoints, while preserving the feedback form.

Improved estimates of the slow adjoints can be obtained by extending the singular perturbation analysis to include first- and higher-order corrections. In [10] the guidance law of Eq.(81) was improved by incorporating first-order corrections , obtained using the method of Matched Asymptotic Expansions (MAE) [22-26], in a feedback form.

In order to demonstrate the improvements that can be obtained by incorporating first-order corrections in the guidance law, an example of a relatively short-range engagement is presented. The conditions and results for this example are summarized in Table 2.

Table 1 Comparison of Exact and Approximate Solutions for a Medium-range Example in the Horizontal Plane

target	$h_T = 12000$ m $V_T = 300$ m/s		
initial state	$R_o = 11192$ m $\psi_o = 64.57°$ $V_o = 349.6$ m/s $\chi_o = -89.61°$	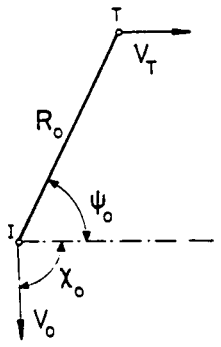	
final state	$R_f = d = 2000$ m		
	exact solution	approx. solution at initial state [Eq. (81), Ref. 10]	approx. solution at initial state [Ref. 13]
"free" final state	$\psi_f = 28.65573°$ $V_f = 455.2$ m/s $\chi_f = 28.65°$	$\bar{V}_f = 436.8$ m/s $\bar{\chi} = 25.45°$	$\bar{V}_f = 605.2$ m/s $\bar{\chi} = 41.69°$
final time	$t_f = 105.0$ s	$\bar{t}_f = 105.2$ s	$\bar{t}_f = 111.2$ s
Interceptor's best turning radius at $V = V_o$: $r_{min} = 2543.5$ m Geometric perturbation parameter (r_{min}/R_o) : $\varepsilon_g = 0.227$			

Table 2 Comparison of Exact and Approximate Solution for a Short-range Example in the Horizontal Plane

target	$h_T = 12000$ m $V_T = 350$ m/s		
initial state	$R_o = 6318.5$ m $\psi_o = 18.87°$ $V_o = 598.2$ m/s $\chi_o = -44.391°$	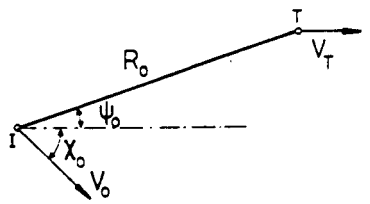	
final state	$R_f = d = 2000$ m		
	exact solution	zeroth-order approx. solution at initial state [Eq. (81), Ref. 10]	first-order approx. solution at initial state [Ref. 10]
"free" final state	$\psi_f = 30.08239°$ $V_f = 543.4$ m/s $\chi_f = 28.65°$	$\bar{V}_f = 600.1$ m/s $\bar{\chi} = 9.6°$	$\bar{V}_f = 555.4$ m/s $\bar{\chi} = 26.2°$
final time	$t_f = 27.0$ s	$\bar{t}_f = 27.8$ s	$\bar{t}_f = 27.1$ s
Interceptor's best turning radius at $V = V_o$: $r_{min} = 7447.2$ m Geometric perturbation parameter (r_{min}/R_o) : $\varepsilon_g = 1.18$			

These results show that in this case with a rather large value of ϵ_g, the payoff error of the zeroth-order approximation is of the order of 3%. The error in the reference (predicted final) values is even larger. The first-order singular perturbation approximation is rather successful in predicting the final values of the state-variables and, as a consequence, it provides an outstanding payoff accuracy even for an engagement starting within the best turning circle of the interceptor.

The improved accuracy comes at the expense of some additional computations. Although in relative terms the first-order algorithm requires about twice as much CPU time as the zeroth-order algorithm, in absolute terms, the overall computational effort is still rather modest.

V. INTERCEPTION IN A VERTICAL PLANE

A. FORMULATION OF THE VERTICAL INTERCEPTION PROBLEM

1. EQUATIONS OF MOTION

The equations of motion for an air-to-air interception confined to a vertical plane are obtained by setting in Eqs.(1-6) $y = 0$. This leads via $F_y = 0$ to $\chi = 0$ (or $\chi = \pi$) and consequently to $\mu = 0$ (or $\mu = \pi$). The resulting equations of motion are:

$$\dot{x} = V\cos\gamma - V_T \triangleq f_x(V,\gamma) \tag{83}$$

$$\dot{h} = V\sin\gamma \triangleq f_h(V,\gamma) \tag{84}$$

$$\dot{V} = g[(nT_{max} - D_0 - n^2 D_i)/W - \sin\gamma] \triangleq f_V(h,V,\gamma,n,n) \tag{85}$$

$$\dot{\gamma} = (g/V)[n - \cos\gamma] \triangleq f_\gamma(V,\gamma,n) \tag{86}$$

In these equations $-\pi \leq \gamma \leq \pi$, which allows both for incoming and outgoing targets (see Fig.3).

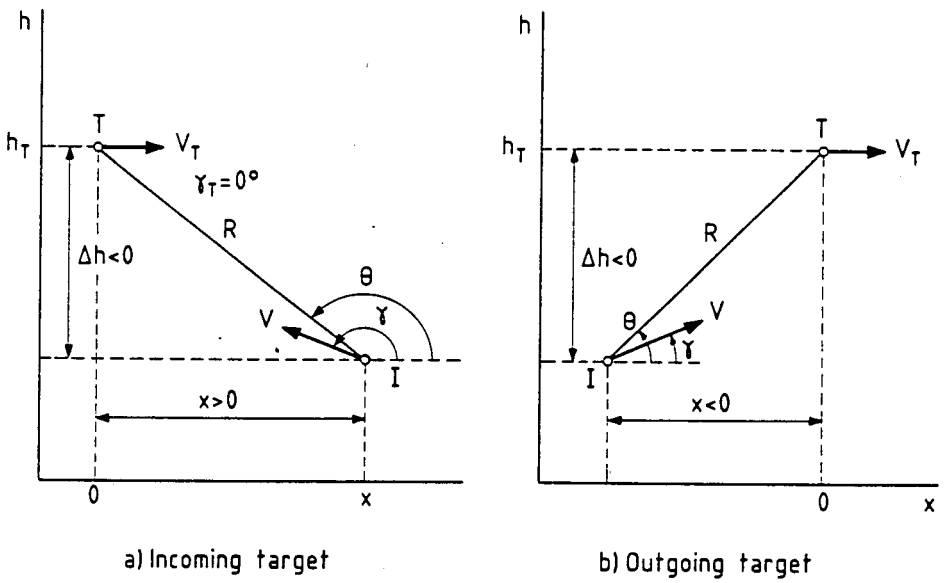

Fig. 3. Vertical Interception Geometries.

In a frequently used alternative formulation the specific energy:

$$E = h + V^2/2g \tag{87}$$

is used as a state variable replacing V, which merely continues to serve as an abbreviation for:

$$V = \{2g(E - h)\}^{1/2} \tag{88}$$

In this case Eq.(85) is replaced by:

$$\dot{E} = [\eta T_{max} - D_0 - n^2 D_i]V/W \triangleq f_E(h,E,\eta.n) \tag{89}$$

In the sequel of this Chapter this "energy-state" formulation is used.

The terminal manifold of the vertical interception is defined by:

$$\Phi = x(t_f)^2 + [\Delta h(t_f)]^2 - d^2 = 0 \tag{90}$$

2. OPTIMAL CONTROL FORMULATION

The variational Hamiltonian for vertical interception is:

$$H = -1 + \lambda_x f_x + \lambda_h f_h + \lambda_E f_E + \lambda_\gamma f_\gamma + \text{constraints} \tag{91}$$

The necessary conditions for optimality include the adjoint differential equations and transversality conditions:

$$\dot{\lambda}_x = -\frac{\partial H}{\partial x} = 0 , \qquad \lambda_x(t_f) = 2\nu x(t_f) \tag{92}$$

$$\dot{\lambda}_h = -\left.\frac{\partial H}{\partial h}\right|_E , \qquad \lambda_h(t_f) = 2\nu\Delta h(t_f) \tag{93}$$

$$\dot{\lambda}_E = -\left.\frac{\partial H}{\partial E}\right|_h , \qquad \lambda_E(t_f) = 0 \tag{94}$$

$$\dot{\lambda}_\gamma = -\frac{\partial H}{\partial \gamma} , \qquad \lambda_\gamma(t_f) = 0 , \tag{95}$$

where:

$$\left.\frac{\partial H}{\partial h}\right|_E = \left.\frac{\partial H}{\partial h}\right|_V - \frac{g}{V}\left.\frac{\partial H}{\partial V}\right|_h \tag{96}$$

and:

$$\left.\frac{\partial H}{\partial E}\right|_h = \frac{g}{V}\left.\frac{\partial H}{\partial V}\right|_h \tag{97}$$

Unfortunately, the adjoint equations of the vertical interception cannot be integrated in a analytical form, as it was done for the horizontal case. The main reason for this difficulty is the dependence of the thrust and the aerodynamic forces on the altitude. However, the optimal control solution, if it exists, can be expressed by using the Maximum Principle in terms of the state and adjoint variables:

$$\lambda_E > 0 : \quad n^* = 1 , \qquad n^* = \min [\ |n_u|, n_{max}]\ \text{sign}(\lambda_\gamma) \tag{98}$$

$$\lambda_E < 0 : \quad n^* = 0 , \qquad n^* = n_{max}\ \text{sign}(\lambda_\gamma) \ , \tag{99}$$

where n_u is the unconstrained optimal load factor given by:

$$n_u = \frac{\lambda_\gamma}{\lambda_E} \frac{W}{2V^2 D_i} \tag{100}$$

A singular throttle arc, along which $\lambda_E = 0$ over a non-zero time interval, is likely to occur only in isolated situations.

Since time is not explicitly involved and the final time is unspecified:

$$H^* = H\Big|_{t_f} = 0 \ , \tag{101}$$

which allows to determine the value of the multiplier ν in Eqs.(92) and (93):

$$\nu = \{[V(t_f)\cos\gamma(t_f) - V_T]x(t_f) + V(t_f)\sin\gamma(t_f)\Delta h(t_f)\}/2 \tag{102}$$

Since at t_f both λ_E and λ_γ vanish, the control at the final time depends upon the derivatives of these variables. Taking the limit of Eq.(100) as $t \to t_f$ results in:

$$\lim_{t \to t_f} n_u = \frac{W}{2D_i} \tan[\theta(t_f) - \gamma(t_f)] \,, \tag{103}$$

where θ is the line of sight angle in the vertical plane (see Fig.3).

B. SINGULAR PERTURBATION ANALYSIS

1. MODELING CONSIDERATIONS

In order to obtain an approximation of the optimal control solution in a feedback form the approach of forced singular perturbation (FSP), outlined in Section III, is to be applied. As a first step in this direction the following observations, referring to the time-scale separation of the state variables, are made:

- The rate of change of the horizontal range component x is rather gradual, suggesting that it should be considered as a slow variable.
- In a medium-range scenario the maximum speed (specific energy) of the interceptor cannot be reached. Therefore, the specific energy has to be considered on the same time-scale as the horizontal range component.
- In most known "energy-state" models altitude is considered as a fast variable compared to the specific energy.
- The flight path angle γ can change much faster than the relative geometry expressed by x and Δh.

In some previous studies [30,34] considerable attention was paid to the coupling between the altitude and the flight path angle, having its origin in the phugoid mode of an uncontrolled aircraft. Full consideration of this coupling leads to analyze both variables on the same time-scale and requires as a consequence to solve a numerically very sensitive two-point boundary value problem. In [5] it was, however, shown that the error induced by neglecting the coupling and analyzing h and γ on

separate time-scales is mainly due to a reduced damping of the resulting second order dynamic response, while the frequency remains almost unchanged. Moreover, it was also reported [5] that this error could be corrected by slightly modifying the cost function. A similar result was achieved by a feedback approximation derived in [11].

Based on the above, the following FSP model is used in the present analysis:

$$\dot{x} = f_x(V,\gamma) \quad , \qquad x(t_0) = x_0 \tag{104}$$

$$\dot{E} = f_E(h,E,n.n) \quad , \qquad E(t_0) = E_0 \tag{105}$$

$$\varepsilon\dot{\Delta h} = f_h(V,\gamma) \quad , \qquad \Delta h(t_0) = h_0 - h_T \tag{106}$$

$$\varepsilon^2\dot{\gamma} = f_\gamma(V,\gamma,n) \quad , \qquad \gamma(t_0) = \gamma_0 \tag{107}$$

The terminal manifold and the variational Hamiltonian remain the same as in Eqs.(90) and (91). The adjoint equations and the transversality conditions corresponding to the FSP model are:

$$\dot{\lambda}_x = -\frac{\partial H}{\partial x} = 0 \quad , \qquad \lambda_x(t_f) = 2\nu x(t_f) \tag{108}$$

$$\dot{\lambda}_E = -\left.\frac{\partial H}{\partial E}\right|_h \quad , \qquad \lambda_E(t_f) = 0 \tag{109}$$

$$\varepsilon\dot{\lambda}_h = -\left.\frac{\partial H}{\partial h}\right|_E \quad , \qquad \lambda_h(t_f) = 2\nu\Delta h(t_f) \tag{110}$$

$$\varepsilon^2\dot{\lambda}_\gamma = -\frac{\partial H}{\partial \gamma} \quad , \qquad \lambda_\gamma(t_f) = 0 \tag{111}$$

2. BASIC GUIDANCE LAW SYNTHESIS

The FSP model, represented by Eqs.(104)-(111), was solved in [11] and is briefly reviewed in the following. By setting $\varepsilon = 0$ in these equations, the "reduced order" problem (the variables are denoted by the superscript "r") with $f_h^r = f_\gamma^r = 0$ is obtained. Consequently, one has:

$$\sin\gamma^r = 0 \tag{112}$$

and:

$$n^r = \cos\gamma^r \tag{113}$$

For an outgoing target ($|\gamma| \leq \pi/2$) this leads to $\gamma^r = 0$ and $n^r = 1$, while for an incoming target ($|\gamma| \geq \pi/2$) $\gamma^r = \pi$ and $n^r = -1$ (see Fig.3).

Substituting these results into Eq.(91) and using Eqs.(101) and (109) leads to:

$$\lambda_x^r = \frac{1}{V_f^r\cos\gamma^r - V_T} = \frac{1}{\pm V_f^r - V_T} \quad , \tag{114}$$

as well as to:

$$\lambda_E^r = \frac{(V_f^r - V^r)\cos\gamma^r}{V_f^r\cos\gamma^r - V_T}\,\frac{1}{f_E^r} = \frac{\pm(V_f^r - V^r)}{\pm V_f^r - V_T}\,\frac{1}{f_E^r} \quad , \tag{115}$$

where V_f^r, the value of V^r at t_f, is an unknown parameter depending on the initial conditions and the prescribed terminal range d. The control variables of the "reduced-order" problem are n^r and h^r. For a successful interception V_f^r must be greater than V_T.

Inside the flight envelope the aircraft can accelerate (i.e., $V_f^r > V^r$ and $f_E^r > 0$), and therefore $n^r = 1$.

Moreover, the optimal altitude is given by:

$$h^r = \arg \{ \max_h \frac{f_E(h, E^r, n=1, n=\pm 1)}{(V_f^r - V^r)} \} \triangleq \tilde{h}^r(E^r, V_f^r) \quad , \tag{116}$$

describing a "reduced-order" optimal flight path in the h-V plane. A family of such flight paths, parameterized by V_f^r is depicted in Fig.4. The value of V_f^r can be obtained, for a given set of initial and terminal conditions, by a fast converging iterative process, called "range matching" [5,11]. It solves the implicit integral equation:

$$|x_0| - d = \left| \int_{E_0}^{E_f} \frac{V^r \cos\gamma^r - V_T}{f_E[\tilde{h}^r(E, V_f^r), E, n=1, n\pm 1]} dE \right| \triangleq I_x(E_0, V_f^r) \quad , \tag{117}$$

where V^r is, based on Eq.(88), a function of E^r and $\tilde{h}^r(E^r, V_f^r)$. The solution yields therefore $V_f^r = \tilde{V}_f^r(x_0, E_0)$, abbreviated in the sequel as $\tilde{V}_f^r$.

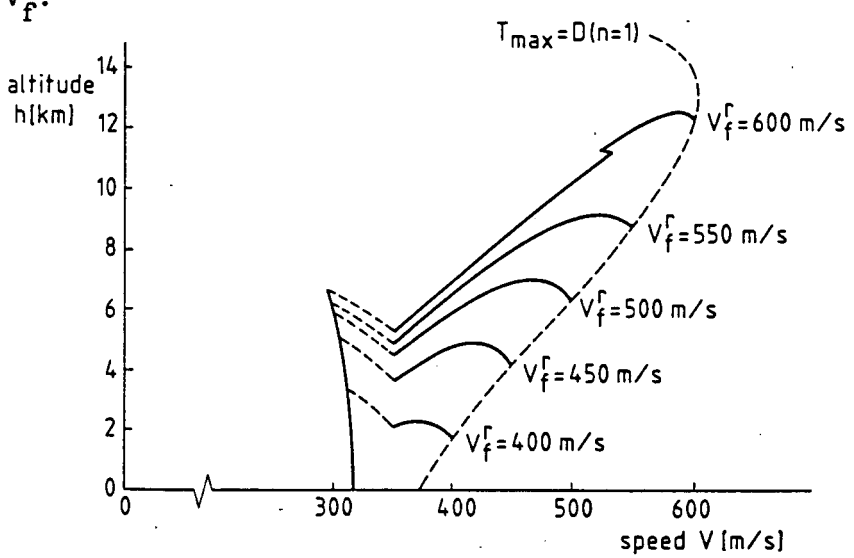

Fig. 4 Family of "Reduced-order" Trajectories in the Vertical Plane

Since the "reduced-order" solution, cannot satisfy the initial conditions of the "fast" variables, Δh and γ, two consecutive boundary layer solutions are needed. Substitution of the stretched time-scale:

$$\tau_1 = (t-t_0)/\varepsilon \quad , \tag{118}$$

into Eqs.(104)-(111) provides the first boundary layer, where the variables are denoted by the superscript "^{1}". By setting $\varepsilon = 0$ in these equations the following results are obtained:

$$x^1(\tau_1) = x_0 , \quad E^1(\tau_1) = E_0 , \quad f_\gamma^1(\tau_1) = 0 \rightarrow \quad n^1 = \cos\gamma^1 \tag{119}$$

$$\lambda_x^1(\tau_1) = \lambda_x^r, \quad \lambda_E^1(\tau_1) = \lambda_E^r(t_0) \rightarrow \quad n^1 = 1, \quad \frac{\partial H}{\partial \gamma}^1 = 0 \tag{120}$$

As a consequence of Eq.(120), the active control in this boundary layer is the flight path angle γ^1 which can be approximated [11] by the following relatively simple feedback form:

$$\gamma^1 = \arccos\left\{\frac{V^1 f_E^r(E_0,\tilde{V}_f^r)}{\tilde{V}_f^r[f_E^r(E_0,\tilde{V}_f^r) - f_E^1(E_0)] + V_0^r f_E^1(E_0)}\right\} \times$$
$$\text{sign}[\tilde{h}^r(E_0,\tilde{V}_f^r) - h^1]$$
$$= \tilde{\gamma}^1(E_0,\tilde{V}_f^r,h^1) \quad , \tag{121}$$

where $f_E^r(E_0,\tilde{V}_f^r)$ is an abbreviation for $f_E[\tilde{h}^r(E_0,\tilde{V}_f^r),E_0,n=1,n=\pm1]$, $f_E^1(E_0)$ is an abbreviation for $f_E(h^1,E_0,n=1,n=\cos\gamma^1)$, and V_0^r is the value of V^r expressed by Eq.(88) at E_0 and $\tilde{h}^r(E_0,\tilde{V}_f^r)$. The active adjoint variable in this boundary layer is approximated by:

$$\lambda_h^1(\tau_1) = \lambda_x^r \tan\gamma^1 \tag{122}$$

In the next boundary layer the time-scale is further stretched:

$$\tau_2 = \tau_1 / \varepsilon \tag{123}$$

Substitution of Eq.(123) into the state and adjoint equations and setting again $\varepsilon = 0$, while denoting the variables of this boundary layer by the superscript "^{2}", yields:

$$x^2(\tau_2) = x_0, \quad E^2(\tau_2) = E_0, \quad h^2(\tau_2) = h_0 \tag{124}$$

$$\lambda_x^2(\tau_2) = \lambda_x^r, \quad \lambda_E^2(\tau_2) = \lambda_E^r(t_0) \;\rightarrow\; n^2 = 1,$$

$$\lambda_h^2(\tau_2) = \lambda_x^r \tan\tilde{\gamma}^1(E_0, \tilde{V}_f^r, h_0) \tag{125}$$

These results allow to obtain a feedback expression for the unconstrained load factor at $\tau_2 = 0$:

$$n_u^2(0) = \cos\gamma_0 + A(E_0, \tilde{V}_f^r, h_0)\, \sin\left[\frac{\tilde{\gamma}^1(E_0, \tilde{V}_f^r, h_0) - \gamma_0}{2}\right]$$

$$= \tilde{n}_u^2(x_0, E_0, h_0, \gamma_0)\,, \tag{126}$$

where:

$$A(E_0, \tilde{V}_f^r, h_0) = \left[\frac{2}{\tilde{V}_f^r - V_0^r} \frac{Wf_E[\tilde{h}^r(E_0, \tilde{V}_f^r), E_0, n=1, n=\cos\tilde{\gamma}^1]}{D_i(E_0, h_0)\, \cos\tilde{\gamma}^1(E_0, \tilde{V}_f^r, h_0)}\right]^{1/2} \tag{127}$$

Based on Eq.(126), a uniformly valid zeroth-order feedback control law can be synthesized by replacing the initial values of the state variables with their current values. Since this guidance law is totally independent of the target trajectory, in [11] an intuitive feedback control was proposed for the terminal phase of the interception.

3. GUIDANCE LAW IMPROVEMENTS

Further analysis [12] revealed several deficiencies and error sources in the guidance algorithm summarized in the previous subsection:

(i) The convergence of the aircraft trajectory guided by Eq.(126) towards the reference trajectory of the "reduced-order" solution is very slow.

(ii) The reference trajectory is discontinuous in the transonic region (the "transonic jump" phenomenon).

(iii) The solution for the terminal phase of the interception (terminal boundary layer) is not satisfactory.

The origin of the first deficiency lies in Eq.(112), obtained for the "reduced-order" solution from $f_h^r = 0$. This result is clearly incompatible with the actual flight path angle associated with the "reduced-order" optimal flight path, defined by Eq.(116). Along every smooth segment of this trajectory the flight path angle is given by:

$$\sin\gamma^R = \frac{T-D}{W}/\left(1 + \frac{V}{g}\frac{dV^r}{dh^r}\right) = \sin\gamma^R(E,V_f^r) \neq 0 \qquad (128)$$

In order to avoid this problem one can follow the approach introduced in [35] and replace the altitude by another "fast" variable Ω, defined as:

$$\Omega \triangleq \frac{\partial}{\partial h}\Big|_E \left\{\frac{f_E}{(V_f - V)\cos\gamma}\right\} = \Omega(h,V,V_f) \qquad (129)$$

This variable reaches an equilibrium on the "reduced-order" optimal trajectory as requested by Eq.(116) and its time derivative is given by:

$$\dot{\Omega} = \frac{\partial\Omega}{\partial h}\dot{h} + \frac{\partial\Omega}{\partial V}\dot{V} = \sin\gamma\left(V\frac{\partial\Omega}{\partial h} - g\frac{\partial\Omega}{\partial V}\right) + \frac{T-D}{W}\,g\frac{\partial\Omega}{\partial V} \triangleq f_\Omega(h,V,\gamma) \qquad (130)$$

Clearly, by replacing Eq.(106) with:

$$\dot{\varepsilon\Omega} = f_{\Omega} \tag{131}$$

and setting $\varepsilon = 0$ one obtains Eq.(128) because:

$$-(\frac{\partial\Omega}{\partial h})/(\frac{\partial\Omega}{\partial V}) = \left.\frac{dV}{dh}\right|_{\Omega} \tag{132}$$

Indeed, by adding γ^R to Eq.(121), i.e. redefining:

$$\gamma^{1*} \triangleq \gamma^1 + \gamma^R \quad , \tag{133}$$

to replace γ^1 in Eqs.(126) and(127), a significant improvement is achieved.

The "transonic jump" is a well known characteristic of most supersonic aircraft. It is the result of the "reduced-order" modeling, where altitude is considered as a pseudo-control and as such the corresponding optimal trajectory can be discontinuous. In the open-loop optimal solution of the complete point-mass model such discontinuity does not exist. In terms of rigorous singular perturbation theory the "transonic jump" has to be treated as an "internal" boundary layer. Such a solution was obtained recently [36], but unfortunately only in an open-loop form. In the frame of a feedback algorithm an acceptable solution is to replace the transonic discontinuity by a continuous reference flight path, such as a backward extrapolation of the supersonic subarc of the "reduced-order" optimal trajectory. Since such a flight path is not optimal in the sense of the "reduced-order" modeling, it may happen that the argument of Eq.(121) is greater than 1. In order to avoid such problem, it was proposed [12] to use instead of Eq (127) another feedback control law:

$$n_u(E,x,h,\gamma) = \cos\gamma + \{\omega^2[h^r_{ex}(E,x)-h] + 2V\zeta\omega[\gamma^R_{ex}(E,x)-\gamma]\}/g \ , \quad (134)$$

where $h^r_{ex}(E,x)$ and $\gamma^R_{ex}(E,x)$ are values obtained from the extrapolated supersonic subarc. In this expression ω and ζ are control parameters associated with the linearized second-order response of the aircraft. For the damping ratio the value of $\zeta = 0.7$ was selected, while ω was obtained by some numerical experimentation for an optimal performance. For several aircraft models the best value of ω was in the range of 0.08 - 0.15.

The two modifications, which are outlined above, created an improved feedback control algorithm for steering the interceptor towards the "reduced-order" flight path asymptotically. This algorithm, being independent of the target altitude, cannot guarantee that the terminal manifold of Eq.(90), which involves a "fast" variable, is reached. This is an inherent limitation of a "reduced order" solution, to which singular perturbation theory provides an answer in the form of a "terminal" boundary layer. Such a "terminal" boundary layer solution imposes two difficulties. It must be stable in a reversed stretched time-scale [37], which means a structural instability in a real-time (forward) implementation. Another difficulty is to determine the point of transition for starting the "terminal" boundary layer solution.

If the target altitude is lower than the final part of the "reduced-order" trajectory, the terminal phase of the time-optimal interception is a dive along the maximum dynamic pressure limit. This type of trajectories were treated extensively in [3-5]. In other investigations [11-14] the attention is focused on interception of high flying targets. In such a situation the classical energy-state approximation [1] calls for a "zoom" climb at a constant specific energy until the terminal manifold is reached.

In [12] a closed form analytical solution for such "zoom" trajectory is derived and proposed as an approximation for the "terminal" boundary layer solution of the minimum-time interception in the vertical plane. The derivation of this closed form solution is summarized in the Appendix. Here the main results are repeated, denoting the variables of the constant specific energy "zoom" by the superscript "z".

The solution is characterized by:

$$V^z/\cos\gamma^z = V(t_f)/\cos\theta(t_f) = A_f \tag{135}$$

and the nominal load factor to generate the trajectory is given by:

$$n^z = 2\cos\gamma^z \tag{136}$$

The "zoom" trajectory can be completely determined by the closed form solution. Thus, the unknown constant A_f, the starting time t_0^z and the corresponding horizontal distance $x(t_0^z)$ can be found. At the same time the entire "zoom" trajectory can be precomputed and stored. Since the closed form solution is only an approximation one must monitor the deviation of the actual trajectory and correct it. For this purpose the following feedback control law, motivated by Eq.(103), has been proposed:

$$n(t \geq t_0^z) = 2\cos\gamma + \frac{W}{2D_i}\tan[\,\gamma^z(\theta) - \gamma\,] \tag{137}$$

By incorporating the appropriate corrections to all three deficiencies, mentioned at the beginning of this subsection, a modified feedback control algorithm was synthesized [12]. It was also demonstrated [12] that this new algorithm leads to improvements of the order of 1% in the pay-off in comparison with the uncorrected guidance law.

4. ACCURACY ASSESSMENT

The absolute pay-off accuracy of the improved guidance algorithm was tested by a comparison with the open-loop optimal solution obtained by a very accurate numerical multiple shooting method [14]. In the numerical examples an unclassified F-4 type model was used. This comparison, which is summarized in Table 3, demonstrated a rather satisfactory pay-off accuracy of the "original" FSP solution, in the order of 1% .

Table 3 Comparison of Interception Time in the Exact and Approximate Solutions for Medium-range Examples in the Vertical Plane

initial state	$R_o = 82800$ m $V_o = 250$ m/s $\gamma_o = 180°$ (incoming target) $h_o = 1000$ m			
final state	$R_f = d = 1000$ m			
example No.		1	2	3
target	h_T (m)	4180	7000	12000
	V_T (m/s)	300	300	400
interception time (s)	exact solution	122.78	124.03	113.99
	original FSP sol.	123.56	124.86	115.02
	modified FSP sol.	122.88	124.26	114.54

The comparison revealed, however, a discrepancy between the FSP and the optimal trajectories in the subsonic region. There is a clear indication, as can be seen in Fig.5, that the subsonic subarc of the reduced-order trajectory is far from "optimal". The subsonic subarc in the reduced-order solution features a constant Mach number of M = 0.92 up to an altitude of about 5 km, where the "transonic jump" starts. In contrast, the open-loop optimal trajectory is an accelerating climb into the supersonic region. The origin of this nonoptimality is the incompatibility of the assumption of $|\cos\gamma^r| = 1$, imbedded in the "reduced-order" optimization, and Eq.(128) which predicts flight path angles of the order of 30÷35 degrees in the subsonic region. In the supersonic region, the flight paths angles generally do not exceed 5-6 degrees and the assumption of $|\cos\gamma^r| = 1$ remains valid. It is important to note, that even if the approach of the modified "fast" variable Ω is used, the value of $\cos\gamma^r$ which maximizes the Hamiltonian will still be 1.

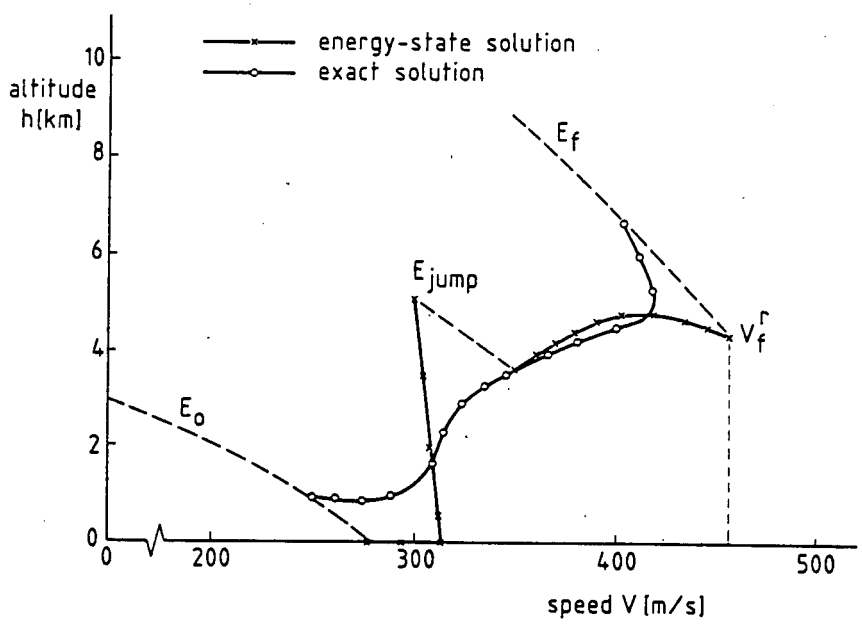

Fig. 5. Non-optimality of the Subsonic Subarc (F-4 model).

The practical conclusion drawn from this comparison has been that the "reduced-order" subsonic subarc should not be used as a reference trajectory for the FSP feedback algorithm. This conclusion is entirely compatible with the previously introduced correction in the transonic region. As an acceptable reference trajectory for the sub and transonic regions a smooth flight path, which starts at zero altitude and blends into the supersonic subarc of the "reduced-order" trajectory,has been proposed [38]. Such a modification reduced the error of the FSP feedback approximation for the medium-range interception in the vertical plane to be less than 0.5%.

VI. THREE-DIMENSIONAL INTERCEPTION

A. MODELING CONSIDERATIONS

Since the FSP models used for the interception in the horizontal and the vertical planes are different, the extension of these feedback algorithms to a three-dimensional scenario is by no means trivial. In [4-6] it was assumed that the azimuth angle χ is a slower variable than the altitude and the flight path angle γ. This assumption, however, has not been confirmed by the results obtained in these very works. It turns out that all three-dimensional interceptions are composed of two phases: a relatively brief initial turning phase followed by an interception in the vertical plane. This observation seems to suggest that χ is a faster variable than h and γ.

In other works [13,14] it was claimed that since horizontal and vertical turning rates are the components of the same physical quantity,- namely the total turning rate of the velocity vector,- both χ and γ have to be analyzed on the same time-scale. This approach is adopted here in the sequel.

The FSP model, proposed for the analysis of the three-dimensional interception, incorporates also the replacement of the

altitude by $Q(h,V)$ defined by Eq.(129) and it is given as follows:

$$\dot{x} = F_x \quad , \qquad x(t_0) = x_0 \tag{138}$$

$$\dot{y} = F_y \quad , \qquad y(t_0) = y_0 \tag{139}$$

$$\dot{E} = F_E = f_E \quad , \qquad E(t_0) = h_0 + V_0^2/2g \tag{140}$$

$$\varepsilon\dot{Q} = F_Q = f_Q \quad , \qquad Q(t_0) = Q(h_0, V_0) \tag{141}$$

$$\varepsilon^2\dot{\gamma} = F_\gamma \quad , \qquad \gamma(t_0) = \gamma_0 \tag{142}$$

$$\varepsilon^2\dot{\chi} = F_\chi \quad , \qquad \chi(t_0) = \chi_0 \quad , \tag{143}$$

with the terminal manifold:

$$\Phi = x(t_f)^2 + y(t_f)^2 + [\Delta h(t_f)]^2 - d^2 = 0 \tag{144}$$

The corresponding variational Hamiltonian is:

$$H = -1 + \lambda_x F_x + \lambda_y F_y + \lambda_E F_E + \lambda_Q F_Q + \lambda_\gamma F_\gamma + \lambda_\chi F_\chi + \text{constraints} \tag{145}$$

The adjoint differential equations and transversality conditions are:

$$\dot{\lambda}_x = -\frac{\partial H}{\partial x} = 0 \quad , \qquad \lambda_x(t_f) = 2\nu x(t_f) \tag{146}$$

$$\dot{\lambda}_y = -\frac{\partial H}{\partial y} = 0 \quad , \qquad \lambda_y(t_f) = 2\nu y(t_f) \tag{147}$$

$$\dot{\lambda}_E = -\left.\frac{\partial H}{\partial E}\right|_{\Omega} \quad , \qquad \lambda_E(t_f) = 0 \tag{148}$$

$$\varepsilon\dot{\lambda}_\Omega = -\left.\frac{\partial H}{\partial \Omega}\right|_{E} \quad , \qquad \lambda_\Omega(t_f) = 2v[\Delta h(t_f)]/\left.\frac{\partial \Omega}{\partial h}\right|_{E(t_f)} \tag{149}$$

$$\varepsilon^2\dot{\lambda}_\gamma = -\frac{\partial H}{\partial \gamma} \quad , \qquad \lambda_\gamma(t_f) = 0 \tag{150}$$

$$\varepsilon^2\dot{\lambda}_\chi = -\frac{\partial H}{\partial \chi} \quad , \qquad \lambda_\chi(t_f) = 0 \tag{151}$$

B. GUIDANCE LAW SYNTHESIS

Based on the this FSP model the feedback guidance law for three-dimensional interception is synthesized by following the approach outlined in [14], [38] and [39]. The solution of the "reduced-order" problem (obtained by setting $\varepsilon = 0$), provides a "required flight trajectory" (RFT). This trajectory lies in a vertical plane. Using Eqs.(151), (146) and (147), the orientation of this plane can be established:

$$\tan \chi^r = y(t_f)/x(t_f) = \text{constant} \tag{152}$$

This "reduced-order" solution is based on a three-dimensional "range matching" process using Eqs.(64-65), with the integrals I_t and I_s evaluated along the RFT, while the velocity is replaced by the specific energy as the independent variable. As the outcome of this process the values of the constants χ^r and V_f^r as well as the RFT profile, defined by $\tilde{h}^r(E,V_f^r)$, and $\gamma^R(E,V_f^r)$ are obtained. Based on the experience gained in [14], two alternative approaches can be proposed for obtaining the RFT profile for any given V_f^r.

In the first approach the RFT profile is composed of the supersonic subarc of the "energy state approximation", defined by Eq.(116), and a smooth extrapolation back to the initial point of

the subsonic subarc at sea level. The second alternative is to compute the open-loop optimal trajectory based on an "exact" point-mass aircraft model in the vertical plane, between the same initial point and the prescribed terminal velocity V_f^r on the maximum speed boundary. The initial and terminal flight path angles have to be selected such as to satisfy (at least approximately) $n = \cos\gamma$.

The use of point-mass extremals to build up a family of reference trajectories was motivated by the perturbation feedback scheme of [40]. Although the guidance law of [40] has not been formally derived using singular perturbation analysis, it makes use of singular perturbation ideas in terms of an assumed hierarchical trajectory-family (i.e. boundary-layer) structure. Considering, for instance, guidance in the vertical plane, the feedback law of [40] provides optimal altitude/path-angle transients that funnel into a single energy-range climb path (RFT). In fact, the structure of the vertical guidance law in [40] is identical to the one given by Eq.(134), except that in [40] the feedback gains (and thus ζ and ω) are specified as a function of specific energy, ensuring optimal transient behavior.

In both cases the practical approach is to precompute and store a sufficiently large family of reference trajectories, parameterized by V_f^r. Though the "range matching" is an iterative process, - a one dimensional search for the appropriate value of V_f^r to satisfy Eqs.(64-65), - it converges rapidly and is compatible with a real time on-line implementation.

The other element of the guidance law synthesis consists of determining the actual aircraft controls in order to reach the RFT and tracking it until the terminal phase of the interception starts. If one assumes that the coupling between horizontal and vertical turning maneuvers can be neglected, both turning rates can be optimized independently. This is an important simplification, which allows to compute the horizontal and vertical components of the required load factor separately by using explicit

feedback expressions obtained in the planar analyses. The horizontal load factor component n_h, defined by Eq.(17), is computed using Eq.(81) by replacing the initial conditions with the current value of the state variables as well as $\bar{x}$ and $\bar{V}_f$ with x^r and V_f^r. The vertical load factor component n_v, defined by Eq.(18), is computed by using Eqs.(116), (121), (126) and (133), similarly replacing all initial conditions with the current values of the state variables. The bank angle μ, to be used as the guidance command is given by:

$$\mu = \arctan (n_h/n_v) \quad , \tag{153}$$

while the resultant load factor is expressed as:

$$n = \min \{n_u, n_{max}, n_L\} \quad , \tag{154}$$

where:

$$n_u = [n_v^2 + n_h^2]^{1/2} \quad , \tag{155}$$

as shown in Fig.6.

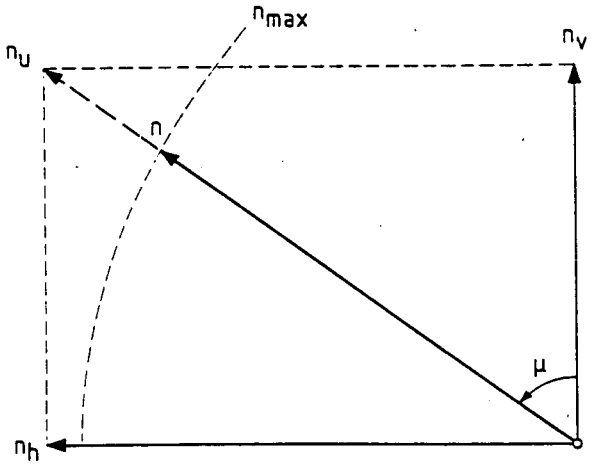

Fig. 6. Three-dimensional Load Factor Synthesis.

In order to test the accuracy of the three-dimensional FSP feedback control synthesis, several examples were computed in [14] and [38]. The results of the comparison to the exact open-loop optimal solution were equally encouraging. They confirmed the validity of the assumption for neglecting the coupling between the horizontal and vertical turning maneuvers in a medium-range scenario. They also demonstrated that the three-dimension feedback algorithm has about the same pay-off accuracy of 1% as the one for vertical interception. Moreover, slight modifications of the algorithm, such as continuous updating of the RFT and correction for the nonoptimality of the subsonic subarc, lead to an improved pay-off accuracy, better than 0.5% .

C. NUMERICAL EXAMPLE

All numerical examples presented thus far, make use of the same aircraft model, which is representative of a previous generation fighter aircraft (F-4). It seems therefore appropriate to evaluate at the present time the accuracy of the FSP feedback approximation on the basis of a more advanced fighter aircraft, featuring a relatively high thrust-to-weight ratio. For this reason, a new numerical example is presented in this subsection, based on an unclassified approximation of a F-15 aircraft model, taken from [40].

A comparison of the solutions based on an "exact" set of point-mass equations of motion with "reduced-order" model solutions has revealed that the influence of the neglected dynamics in the reduced-order solution is far more significant in the case of the F-15 than for the F-4 aircraft model. Figure 7 presents a typical example of such a comparison of the full and reduced-order solutions for the F-15 model. The results clearly indicate that the reduced-order solution is hardly suitable to serve as a RFT in a feedback guidance scheme.

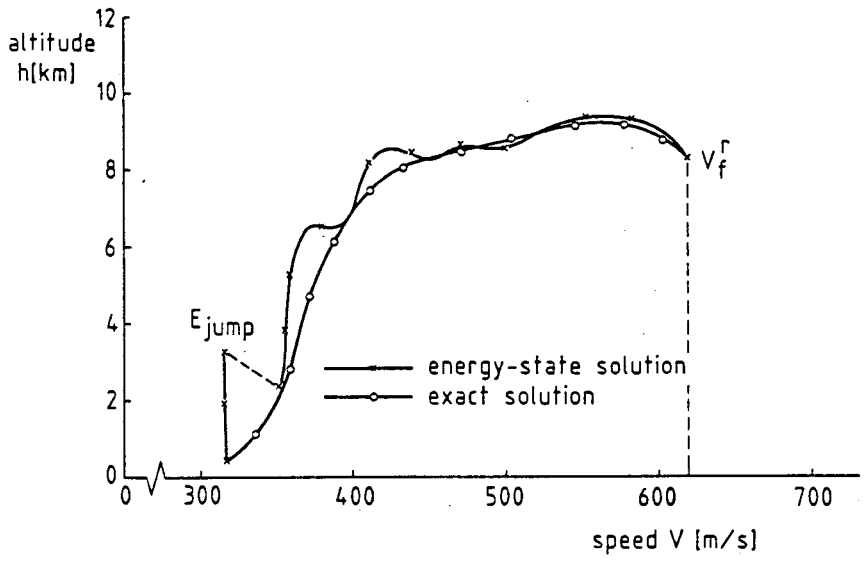

Fig. 7. Full and "Reduced-order" Solutions (F-15 model).

For this reason the approach to the digital simulation of the FSP guidance laws driving the F-15 point-mass system model, has been to store a one-parameter family of precomputed full-order point-mass reference trajectories. The "range matching" feature of the algorithm is then used to select (on-line) the appropriate member of this reference family, to serve as a RFT.

The use of point-mass solutions for serving as RFT, turned out to have the additional advantage that, since no failures of the vertical FSP law could be observed, there was no need to resort to the guidance law of Eq.(134) in the transonic region.

The initial conditions for the example, as well as some important results, are given in Table 4. The example is characterized by a low initial speed and altitude and a relatively large heading error for the interceptor. Figure 8 shows that the initial conditions of the interceptor in the (V,h)-plane are close to the corner velocity locus, implying that the interceptor is capable of achieving relatively high turn rates in the initial phase. As a result, the heading error is corrected very rapidly

(in fact, 90% of the horizontal turn is completed within 15 seconds!). The ground track of the initial turn is shown in Fig.9. Note that the projection of the target velocity vector on the horizontal plane is aligned with the X-axis of the coordinate frame. As heading error is decreased, the emphasis shifts towards high energy and range rates and the control actions are such that the flight is directed towards the RFT. In this transient flight, the interceptor executes a dive in order to gain speed, as can be seen in Fig.8, as well as in Figs.10 and 11. Also note in Fig.11, the rather large rate-of-change of the path-angle in the initial phase, typical of a high performance fighter. Since the target is flying at a relatively high altitude (some 2000 m above the RFT), a zoom climb is commanded in the terminal phase.

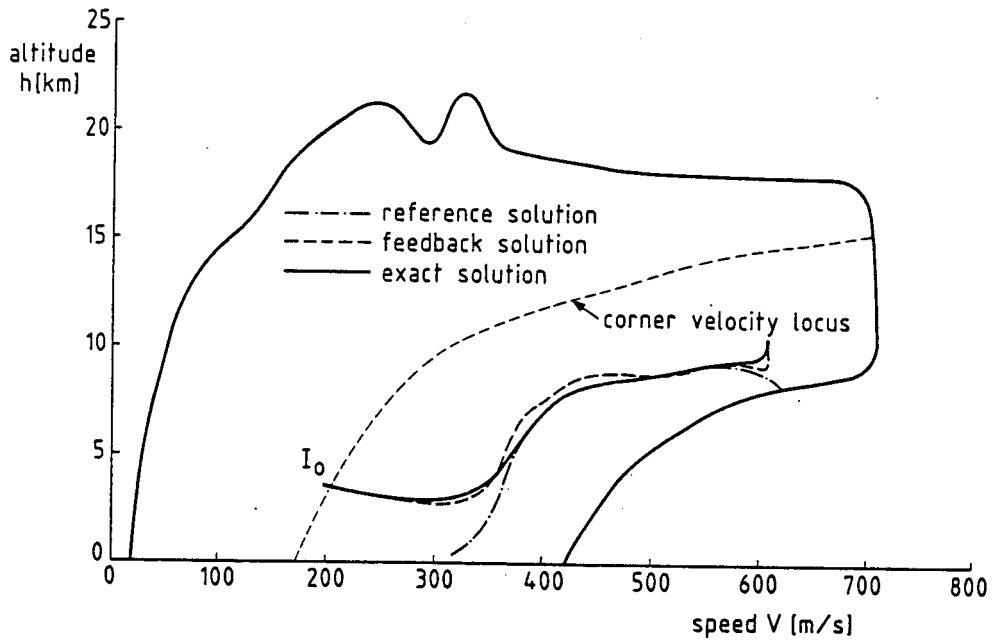

Fig. 8. Comparison of Interceptor Trajectories in the h-V plane.

Table 4. Comparison of Exact and Approximate Solutions for a Three-dimensional Medium-range Example

target	$h_T = 11278$ m $V_T = 200$ m/s		
initial state	$R_o = 47424$ m $\Psi_o = -1.88°$ $\Delta h_o = -7778$ m $V_o = 200$ m/s $\gamma_o = 0°$ $\chi_o = -120°$		
final state	$R_f = d = 3048$ m		
		exact solution	FSP feedback solution
"free" final state	Ψ_f (°)	0.0	0.2
	Δh_f (m)	-738.4	-878.1
	V_f (m/s)	609.0	606.0
	γ_f (°)	10.7	14.9
	χ_f (°)	0.0	0.2
final time	t_f (s)	174.0	174.65

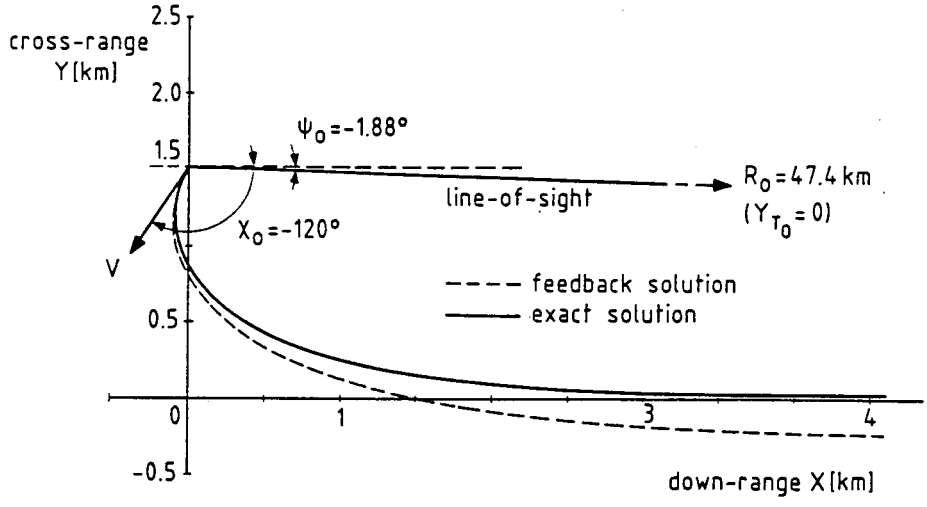

Fig. 9. Comparison of Horizontal Trajectory Projections.

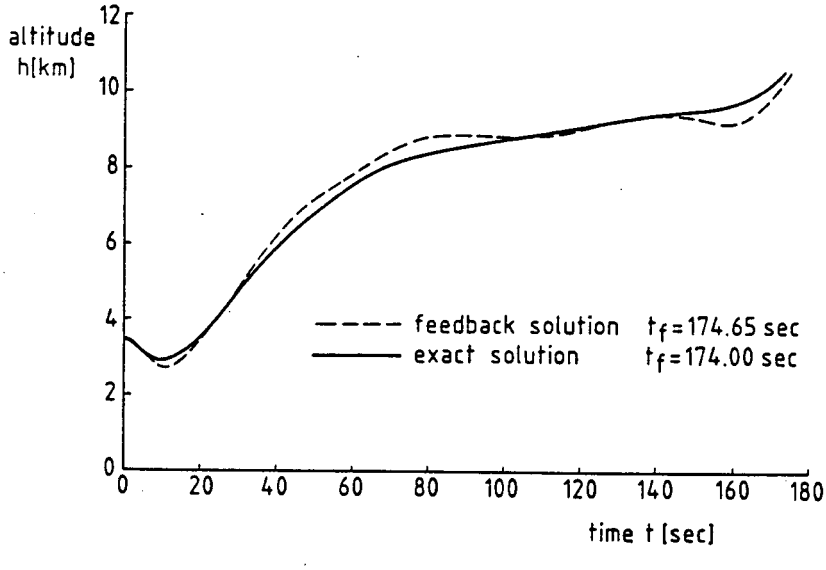

Fig. 10. Comparison of Altitude Time Histories.

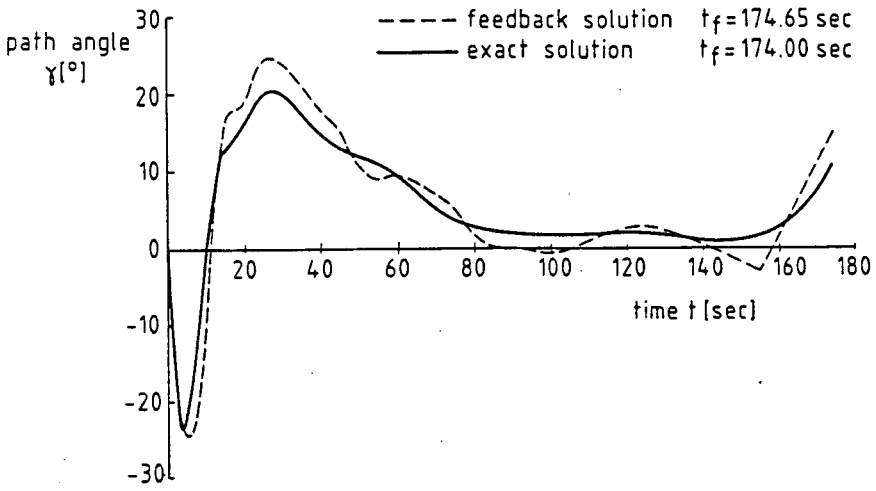

Fig. 11. Comparison of Flight Path Angle Time Histories.

In Figs.8 through 11, a comparison of the simulated feedback solution and the exact open-loop solution is given. The correspondence between the two solutions is remarkably close. As a result, the difference in time-of-capture between the optimal solution and the feedback approximation is only about 0.65 sec (or 0.4%). About 30% of this error can be attributed to the non-optimality of the terminal zoom maneuver and approximately 60% to the initial turning maneuver. It can be concluded that the pay-off accuracy of the FSP feedback guidance law is very satisfactory, even for highly "dynamic" maneuvers, such as the one demonstrated in the present F-15 example.

VII. CONCLUSIONS

In this report an extensive investigation, oriented towards the synthesis of a feedback guidance law for an interceptor aircraft in a medium-range scenario, is summarized. The guidance algorithm is based on the application of a singular perturbation approach. It is composed of two major elements. A fast converging iterative algorithm provides a three-dimensional "reference flight trajectory" (RFT). It is the solution of a "reduced-order" problem, where the interceptor velocity vector can be instantaneously oriented towards the optimal direction. The RFT is tracked by using two feedback control laws for steering the velocity vector in the horizontal and the vertical planes.

In all phases of the reported multi-year investigation the results, obtained by this zeroth-order feedback approximation of the optimal control, were compared with the "exact" (open-loop) optimal solution. This process allowed to introduce modifications in the suboptimal solution leading to a very satisfactory (better than 0.5%) pay-off accuracy.

The new example incorporated in this Chapter, featuring an F-15 aircraft model, has demonstrated the structural robustness of the feedback guidance law. Though in generating the RFT the computational scheme had to be fitted to the aircraft model characteristics, the feedback guidance formulae have remained unchanged.

The feedback algorithm presented here can be distinguished from similar works reported in the open literature by the following:

(i) It incorporates all phases of an air-to-air interception by providing a closed form approximation to the terminal zoom trajectory.

(ii) It has been validated by using different aircraft models and demonstrated a very satisfactory pay-off accuracy, better than any known result in the open literature.

The hierarchical structure of the algorithm, the explicit feedback form of the control laws and the validated high accuracy make it a very attractive candidate for a real-time implementation on board of a future interceptor aircraft.

REFERENCES

1. A.E. Bryson, M.N. Desai and W.C. Hoffman, "Energy-state Approximation in Performance Optimization of Supersonic Aircraft," J. Aircraft, 6, 481-488 (1969).
2. R.L. Schultz and N.R. Zagalsky, "Aircraft Performance Optimization," J. Aircraft, 9, 108-114 (1972).
3. A.J. Calise and D.D. Moerder, "Singular Perturbation Analysis of Minimum-time Long Range Intercept," Drexel University Report (1978).
4. R.K. Mehra, R. Washburn, S. Sajan and J. Caroll, "A Study of Application of Singular Perturbation Theory," NASA CR-3167 (1979).
5. A.J. Calise and D.D. Moerder, "Singular Perturbation Techniques for Real-time Aircraft Trajectory Optimization and Control," NASA CR-3597 (1982).
6. D.B. Price, A.J. Calise and D.D. Moerder, "Piloted Simulation of an Onboard Trajectory Optimization Algorithm," J. Guidance and Control, 7, 335-360 (1984).

7. F.P. Jones, E.I. Duke and A.J. Calise, "Flight Test Experience from a Three-dimensional Optimal Interception of a Maneuvering Target," presented at the Second International Symposium on Differential Game Applications, Williamsburg, Virginia, August 21-22, 1986.

8. H.T. Huynh and D. Moraigne, "Quasi-optimal On-line Guidance Law for Military Aircraft," AIAA Paper No.85-1977-CP, presented at the AIAA Guidance and Control Conference, Snowmass, Colorado, August 19-22, 1985.

9. J. Shinar and A. Merari, "Aircraft Performance Optimization By Forced Singular Perturbations," Proc. 12th ICAS Congress, Munich W.Germany, 758-772 (1980).

10. H.G. Visser and J. Shinar, "A Highly Accurate Feedback Approximation for Horizontal Variable Speed Interceptions," J. Guidance, Control and Dynamics, 9, 691-698 (1986).

11. J. Shinar and M. Negrin, "An Explicit Feedback Approximation for Medium-range Interceptions in a Vertical Plane," Optimal Control Applications & Methods, 4, 303-323 (1983).

12. J. Shinar and V. Fainstein, "Improved Feedback Algorithms for Optimal Maneuver in a Vertical Plane," AIAA Paper No.85-1976-CP, presented at the AIAA Guidance and Control Conference, Snowmass, Colorado, August 19-22, 1985.

13. J. Shinar, M. Negrin, K. H. Well and E. Berger, "Comparison Between the Exact and a Approximate Feedback Solution for Medium Range Interception Problems," Proc. of the 1981 Joint Automatic Control Conference, TA-1A (1981).

14. J. Shinar, K.H. Well and B. Jarmark, "Near Optimal Feedback Control for Three-dimensional Interceptions," Proc. of the 15th ICAS Congress, 161-171 (1986).

15. A. Erdelyi, "Singular Perturbations," Bull. Amer. Math. Soc., 68, (1962).

16. S. Kaplan, "in "Fluid Mechanics and Singular Perturbations," (D. A. Lagerstrom, L.N. Howard and C.S. Lin, eds.), Academic Press, New York, 1967.

17. R.E. O'Malley, "Introduction to Singular Perturbations," Academic Press, New York, 1974.

18. R.E. Meyer and S.V. Parter, eds. "Singular Perturbations and Asymptotics," Academic Press, New York, 1980.

19. J. Keworkian and J. Cole, "Perturbation Methods in Applied Mathematics," Springer Verlag, New York, 1980.

20. W. Wasow, "Asymptotic Expansions for Ordinary Differential Equations," Interscience, New York, 1965.

21. W. Eckhaus, "Matched Asymptotic Expansions and Singular Perturbations," North Holland, Amsterdam, 1973.

22. C.R. Hadlock, " The Existence and Dependence on a Parameter of Solutions of a Nonlinear Two Point Boundary Value Problem," J. Differential Equations, 14, (1973).

23. R.R. Wilde and P.V. Kokotovic, "Optimal Open and Closed Loop Control of Singularly Perturbed Linear Systems," IEEE Trans. Automat. Contr., AC-18, (1973).

24. M.I. Freedman and J.L. Kaplan, "Singular Perturbations of Two Point Boundary Value Problems Arising in Optimal Control," J. Optimiz. Theory Appl., 19, (1976).

25. M.D. Ardema, ed., "Singular Perturbations in Systems and Control," Springer Verlag, New York (1982).

26. P.V. Kokotovic, H.K. Khalil and J. O'Reilley, "Singular Perturbation Methods in Control: Analysis and Design," Academic Press, New York, 1986.

27. A.J. Calise, "Singular Perturbation Methods for Variational Problems in Aircraft Flight," IEEE Trans. Automat. Contr., AC-21 (1976).

28. J. Shinar, "On Applications of Singular Perturbation Techniques in Nonlinear Optimal Control," Automatica, 19, 203-211 (1983).

29. J.V. Breakwell, J. Shinar and H.G. Visser, "Uniformly Valid Feedback Expansions for Optimal Control of Singularly Perturbed Dynamic Systems," J.Optimiz. Theory Appl., 46, 441-454 (1985).

30. H.J. Kelley, "in "Control and Dynamic Systems," (C.T. Leondes, ed.), Vol.10, p. 131-178, Academic Press, New York, 1973.

31. H.G. Visser and J. Shinar, "First-order Corrections in Optimal Feedback Control of Singularly Perturbed Nonlinear Systems," IEEE Trans. Automat. Contr., AC-31, 387-393 (1986).

32. N. Rajan, U.R. Prasad and N.J. Rao, "Pursuit-Evasion of Two Aircraft in the Horizontal Plane," J. Guidance and Control, 3, 261-267 (1980).

33. A.J. Calise, "Optimal Thrust Control with Proportional Navigation Guidance,". J. Guidance and Control, 3, 312-318 (1980).

34. M.D. Ardema, "Solution of Minimum Time to Climb Problem by Matched Asymptotic Expansions," AIAA J., 14, 843-850 (1976).

35. H.J. Kelley, E.M. Cliff and A.R. Weston, "Energy State Revisited," Optimal Control Applications & Methods, 7, 195-200 (1986).

36. M.D. Ardema and L. Yang, "Interior Transition Layers in Flight Path Optimization," J. Guidance, Control and Dynamics, 11, 12-18 (1988).

37. A.B. Vasileva, "Asymptotic Solutions of Two Point Boundary Layer Problems for Singularly Perturbed Conditionally Stable Systems, "in "Singular Perturbations: Order Reduction in Control System Design," p. 57-62, ASME, New York, 1972.

38. A. Spitzer, "Development of an Autonomous Guidance for an Aircraft in Air-to-Air Missions," M.Sc. Thesis, Department of Aeronautical Engineering, Technion, Israel Institute of Technology, 1988.

39. J. Shinar, "Concept of Automated Aircraft Guidance System for Air-to-Air Missions," AIAA Paper No.86-2285-CP presented at the 13th Atmospheric Flight Mechanics Conference, Williamsburg, Virginia, August 18-20, 1986.

40. H.G. Visser, H.J. Kelley and E.M. Cliff, " Energy Management of Three Dimensional Minimum Time Intercept," J. Guidance, Control and Dynamics, 10, 574-580 (1987).

APPENDIX: TIME-OPTIMAL ZOOM INTERCEPTION AT CONSTANT SPECIFIC ENERGY

This is an idealized version of the terminal phase of a minimum-time interception in a vertical plane obtained by assuming that the specific energy of the interceptor aircraft is constant and the flight path angle γ is a control variable. In order to avoid confusion, the variables in this simplified model are denoted by a superscript "z". Thus, the first assumption is expressed by:

$$h^z + (V^z)^2/2g = E^z = \text{constant} \tag{156}$$

As a consequence, the velocity V^z is not an independent variable, but merely an abbreviation for:

$$V^z = [2g(E^z - h^z)]^{1/2} \tag{157}$$

By considering the flight path angle γ as a control variable, the following "reduced-order " dynamic system, starting to operate at t_0^z is obtained:

$$\dot{x}^z = V^z \cos\gamma^z - V_T \,, \qquad x(t_0^z) = x_0^z \tag{158}$$

$$\dot{h}^z = V^z \sin\gamma^z \,, \qquad h(t_0^z) = h_0^z \tag{159}$$

The terminal conditions of the interception are derived from Eq.(90) in polar coordinates (being identical to the terminal

conditions of the full order problem they are not indexed by a superscript):

$$x^z(t_f) = - d \cos\theta_f \tag{160}$$

$$h^z(t_f) = h_T - d \sin\theta_f \quad , \tag{161}$$

where θ_f, the direction of the line of sight at t_f, is an unspecified parameter.

The variational Hamiltonian of the time-optimal interception for this simplified model is:

$$H^z = -1 + \lambda_x^z(V^z \cos\gamma^z - V_T) + \lambda_h^z(V \sin\gamma^z) \tag{162}$$

The adjoint equations and the corresponding transversality condition are:

$$\dot{\lambda}_x^z = - \frac{\partial H^z}{\partial x^z} = 0 \quad , \quad \lambda_x^z = \lambda_x^z(t_f) = 2\nu\, x^z(t_f) = -2\nu\, d \cos\theta_f \tag{163}$$

$$\dot{\lambda}_h^z = - \frac{\partial H^z}{\partial h^z}\bigg|_{E^z} = - \frac{g}{V^z} (\lambda_x^z \cos\gamma^z - \lambda_h^z \sin\gamma^z) \quad ,$$

$$\lambda_h^z(t_f) = 2\nu\, [h^z(t_f) - h_T] = -2\nu\, d \sin\theta_f \tag{164}$$

The optimal flight path angle for this "zoom" maneuver, which maximizes the Hamiltonian is:

$$\gamma^z = \arctan (\lambda_h^z / \lambda_x^z) \tag{165}$$

Since time is not explicitly involved and the final time is unspecified one also has:

$$H^z = 0 \tag{166}$$

and consequently, since due to Eq.(165) $\gamma^z(t_f) = \theta_f$:

$$\nu = -1/2d[V^z(t_f) - V_T\cos\theta_f] \tag{167}$$

By substituting Eqs.(163),(166) and (167) into Eq.(162) one obtains for all $t \geq t_0^z$:

$$V^z(\lambda_x^z\cos\gamma^z + \lambda_h^z\sin\gamma^z) = V^z(t_f)/[V^z(t_f) - V_T\cos\theta_f] \tag{168}$$

Since Eq.(165) implies that:

$$\lambda_x^z = G(t)\cos\gamma^z \tag{169}$$

and:

$$\lambda_h^z = G(t)\sin\gamma^z \tag{170}$$

Substitution of these expressions into Eq.(168) yields:

$$G(t) = V^z(t_f)/[V^z(V^z(t_f) - V_T\cos\theta_f)] \quad , \tag{171}$$

as well as:

$$G(t_f) = 1/[V^z(t_f) - V_T\cos\theta_f] \tag{172}$$

Keeping in mind that according to Eq.(163) λ_x^z is a constant, Eqs.(170)-(172) lead to a fundamental relationship which characterizes the minimum-time "zoom" interception at a constant specific energy:

$$V^z/\cos\gamma^z = V^z(t_f)/\cos\theta_f = \text{constant} \triangleq A_f \tag{173}$$

and provide a feedback expression for the optimal control γ^z for any given A_f:

$$\gamma^z = \arccos\,(V^z/A_f) \quad , \tag{174}$$

where V^z represents E^z and h^z via Eq.(156).

From Eq.(174) the rate of change of γ^z and the corresponding load factor n^z can be computed:

$$\dot{\gamma}^z \sin\gamma^z = -(1/A_f)\,\dot{V}\Big|_{E^z} = (g/A_f V^z)\,\dot{h}^z = g\sin\gamma^z/A_f \tag{175}$$

Consequently:

$$\dot{\gamma}^z = g/A_f = \text{constant} \tag{176}$$

By comparing Eq.(86) to Eq.(176) and using Eq.(174) one can directly conclude that:

$$n^z = \cos\gamma^z + (V^z/A_f) = 2\cos\gamma^z \quad , \tag{177}$$

as quoted in Eq.(136).

The closed form solution allows to express the unspecified parameter θ_f as a function of the initial conditions of the "zoom" maneuver E^z, $h(t_0^z)$ and $\gamma(t_0^z)$. Applying Eq.(156) for both the initial and the terminal state and substituting Eq.(161) leads to the following quadratic equation for $\sin\theta_f$:

$$[E^z - h(t_0^z)]\sin^2\theta_f + d\cos^2\gamma(t_0^z)\sin\theta_f + h(t_0^z) - h_T\cos^2\gamma(t_0^z)$$

$$- E^z\sin^2\gamma(t_0^z) = 0 \tag{178}$$

It is easy to see that this equation always has a real positive root (smaller than 1) for any feasible "zoom-climb" trajectory.

Once θ_f is computed from Eq.(178) the terminal altitude can be directly obtained from Eq.(161).

The time required to complete the "zoom" maneuver is derived by using Eq.(176):

$$(t_f - t_0^z) = \frac{1}{g} \frac{V(t_0^z)}{\cos\gamma(t_0^z)} [\theta_f - \gamma(t_0^z)] \tag{179}$$

The corresponding initial horizontal range is obtained by integrating Eq.(158) after the substitution of Eqs.(173)-(176) and using Eqs.(160) and (179):

$$x(t_0^z) = -\frac{1}{2g}\left[\frac{V(t_0^z)}{\cos\gamma(t_0^z)}\right]^2 \left\{[\theta_f - \gamma(t_0^z)] + \frac{1}{2}[\sin(2\theta_f) - \sin(2\gamma(t_0^z))]\right\}$$
$$+ \frac{V_T}{g} \frac{V(t_0^z)}{\cos\gamma(t_0^z)} [\theta_f - \gamma(t_0^z)] x(t_0^z) - d\cos\theta_f \tag{180}$$

Moreover, all the variables along the entire "zoom" trajectory can be expressed as explicit functions of the optimal flight path angle γ^z and the initial conditions. By matching the monotonically varying actual horizontal range x(t) with the result obtained in Eq.(180), the starting time of the "zoom" maneuver t_0^z can be selected and then the entire trajectory can be precomputed and stored. Comparison of the actual and the stored trajectories allows to implement a feedback guidance law as proposed in Eq.(137).